Paleontological Research

Papers in Press

"Papers in Press" includes peer-reviewed, accepted manuscripts of research articles, reviews, and short notes to be published in Paleontological Research. They have not yet been copy edited and/or formatted in the publication style of *Paleontological Research*. As soon as they are printed, they will be removed from this website. Please note they can be cited using the year of online publication and the DOI, as follows:

Humblet, M. and Iryu, Y. 2014: Pleistocene coral assemblages on Irabu-jima, South Ryukyu Islands, Japan. *Paleontological Research*, doi: 10.2517/2014PR020.

doi:10.2517/2017PR020

Integrated Upper Triassic conodont and radiolarian biostratigraphies of the Panthalassa Ocean

DAISUKE YAMASHITA[1], HIKARU KATO[2], TETSUJI ONOUE[3] AND NORITOSHI SUZUKI[2]

[1]*Division of Natural Science, Faculty of Advanced Science and Technology, Kumamoto University, 2-39-1 Kurokami, Chuo-ku, Kumamoto 860-8555, Japan (e-mail: k0231215@kadai.jp)*

[2]*Department of Earth Science, Graduate School of Science, Tohoku University, 6-3 Aramaki aza Aoba, Aoba-ku, Sendai 980-8578, Japan*

[3]*Division of Natural Science, Faculty of Advanced Science and Technology, Kumamoto University, 2-39-1 Kurokami, Chuo-ku, Kumamoto 860-8555, Japan*

Abstract. The Late Triassic conodont biostratigraphy of two pelagic chert sections (sections N and Q) in the Inuyama area, central Japan, was investigated to calibrate the Triassic radiolarian zonation proposed by Sugiyama in 1997 with the conodont zones and the standard Triassic timescale. Based on the stratigraphic distributions of marker species, six conodont zones were defined: the *Paragondolella*? *tadpole* interval Zone, the *Quadralella tuvalica* interval Zone, the *Epigondolella quadrata* interval Zone, the *E.*

***triangularis* interval Zone, the *Mockina postera* interval Zone, and the *M. bidentata* Zone. These conodont zones are comparable to the standard Carnian and Norian conodont zones of North America and the Tethys. The Carnian-Norian boundary in the sections studied is tentatively placed between the last occurrence of a Carnian species (*Q. tuvalica*) and the first occurrences of Norian species (*E. quadrata* and *E. spatulata*). The intercalibrated conodont–radiolarian biostratigraphy from the sections we studied accurately calibrates the radiolarian zones in Japan with standard chronostratigraphic stages and substages.**

Key words: bedded chert, Conodonta, Japan, Panthalassa, Radiolaria, Upper Triassic

Introduction

Triassic pelagic deposits in the Panthalassa Ocean generally consist of cherts that commonly yield radiolarians and conodonts. Because cherts contain no macrofossils, their depositional ages were initially dated using conodonts in the late 1970s and early 1980s (Koike, 1979; Isozaki and Matsuda, 1980, 1982, 1983; Yao *et al*., 1982). However, conodonts are so scarce in cherts that the ages of the deposits were predominantly determined from the radiolarian biostratigraphy, based on an indirect correlation with the ages determined from European and North American radiolarian biostratigraphies (see O'Dogherty *et al*., 2010 for the history of dating the cherts). Despite the poor age control for the cherts, these rocks are suitable

for establishing radiolarian biozones because radiolarians occur continuously in chert sequences. Therefore, many radiolarian biostratigraphies have been established for the Middle and Upper Triassic bedded chert successions in Japanese accretionary complexes (Nakaseko and Nishimura, 1979; Yao *et al*., 1980, 1982; Yao, 1982, 1990; Kishida and Sugano, 1982; Igo and Nishimura, 1984; Kishida and Hisada, 1985, 1986; Sato *et al*., 1986; Yoshida, 1986; Matsuda and Isozaki, 1991; Sugiyama, 1992; Sashida *et al*., 1993; Sugiyama, 1997). One of the landmark papers on pelagic Triassic radiolarian biozones was published by Sugiyama (1997), who established 18 radiolarian zones ranging from the Spathian (late Olenekian) to the end of the Triassic in siliceous rocks in the Inuyama area of central Japan. Sugiyama (1997) determined the total ranges of 247 selected radiolarian taxa with a high-resolution examination of 534 samples from 26 sections along the Kiso River. He correlated them with nine previously reported biozones worldwide and then determined the chronology of the radiolarian zones by compiling previously known age data. This is the most comprehensive study on the subject to date, and the zonation scheme reported is the only one to span almost the whole Triassic with relatively high resolution (O'Dogherty *et al*., 2010). Since Sugiyama's zonation was first applied to sections worldwide, both the standardization of the Triassic timescale and the taxonomy of conodonts have changed significantly. The accurate calibration of chronostratigraphic stages and substages is basically established using ammonites and conodonts (Lucas, 2010), whereas the stratigraphically important conodont genera used to determine these ages with high resolution were only described in the 2000s and 2010s (e.g. Mazza *et al*., 2012b). These advances require that we reexamine the conodont biostratigraphy in

pelagic cherts. The pelagic cherts in Japan are particularly important for reconstructing the paleoclimate and paleoceanography in the pelagic oceans of the Triassic. However, this process is difficult, even if the Triassic stage and substage boundaries have been tentatively assigned to the Triassic bedded chert successions in Japan based on radiolarian biostratigraphy (e.g. Ikeda and Tada, 2014).

In this study, we undertook to establish the conodont biozones in exactly the same sections that Sugiyama (1997) used as the type sections for his radiolarian biozones. Based on the aerial photographs shown by Sugiyama *et al*. (2001), the interval from the lower Carnian to the upper Norian (Upper Triassic) in his sections N and Q were examined to (1) produce a biostratigraphic dataset of conodonts; (2) define the conodont zones based on the occurrence of cosmopolitan species; (3) correlate the conodont zonation defined in this study with the conodont zonations established in North America, the Tethys, and southwest Japan; (4) constrain the Carnian and Norian stage and substage boundaries in the study sections based on these correlations; and (5) refine the ages of the radiolarian zonation proposed by Sugiyama (1997).

Geological setting

Sections N and Q, in which Sugiyama (1997) investigated the radiolarian biostratigraphy, are located in the Inuyama area of central Japan (Figure 1). The sections are part of the Kamiaso Unit (Wakita, 1988), which is regarded as a Jurassic accretionary complex in the Mino Belt.

The Kamiaso Unit consists mainly of Early Triassic 'Toishi-type' siliceous shale, Middle Triassic to Early Jurassic bedded chert, and Middle–Late Jurassic terrigenous clastic rocks. These rocks form the Sakahogi syncline (Mizutani, 1964) and are exposed repeatedly as stacks of thrust sheets on the banks of the Kiso River. Yao *et al*. (1980) identified four chert thrust sheets and labeled them CH-1, CH-2, CH-3, and CH-4 in structurally ascending order. Section N and section Q are situated in different thrust sheets: CH-2 in the northern limb of the Sakahogi syncline and CH-3 in the southern limb, respectively (Figure 1). Paleomagnetic studies have shown that the bedded cherts in sections N and Q accumulated at equatorial latitudes in the Panthalassa Ocean (Shibuya and Sasajima, 1986; Oda and Suzuki, 2000; Ando *et al.*, 2001; Uno *et al*., 2015).

Section N consists mainly of a thick succession of bedded cherts (Figure 2), with a total thickness of 35 m (Figure 3). The section is dominated by B-type red cherts and F-type greenish gray cherts, with several interbedded white cherts (Sugiyama, 1997). The B-type bedded chert shows the clear repetition of distinct siliceous and muddy layers with thicknesses of several centimeters. The F-type (fine-grained quartz) bedded cherts have indistinct boundaries owing to amalgamation.

Two characteristic shale beds, CS-1 and CS-2 (Sugiyama, 1997), are intercalated within section N at 4.4 m and 23.5 m above the section base (Figure 2). These claystone layers can be correlated with layers in section Q (Sugiyama, 1997). An impact ejecta layer (the Sakahogi ejecta layer: Onoue *et al*. 2012, 2016a; Sato *et al*., 2013) has been identified ~50 cm above CS-2 in section N.

Most of the bedded cherts in section Q (ca. 21 m thick) are red, except for the purple cherts in the lowermost part of the section (Figure 4). The stratigraphic interval in the middle part of the section shows strong internal deformation by folding, which suggests a stratigraphic gap in the middle part of the section. A claystone is recognized in CS-1 at 1.4 m above the base of the section. The upper part of the section is intercalated with the CS-2 claystone. However, the Sakahogi ejecta layer cannot be identified in section Q because the bedded cherts above the CS-2 level are strongly deformed (Figure 2).

Material and methods

In this study, we collected 178 chert samples from two sections to produce a biostratigraphic dataset of conodonts. In total, 140 samples were crushed into small pieces and immersed in a 5%–10% solution of hydrofluoric acid in a 100 ml plastic beaker for ca. 10 hour to remove the matrix. The residue was collected with 63 μm and 2 mm meshes, gently rinsed with water, and dried in an oven. The process was repeated more than 10 times to obtain sufficient conodont elements. The specimens were picked with a fine brush under a binocular microscope and photographed digitally with a scanning electron microscope (SEM; JEOL JSM-6360LV).

Conodont biostratigraphy

We present a conodont biostratigraphic record of sections N and Q. These successions yielded early Carnian to late Norian conodonts, which are generally fractured and rare in almost all the samples, especially in the F-type cherts. All the conodonts show a conodont color alteration index (CAI) of 3.0–4.0 on the scale of Epstein *et al*. (1977). We found 27 species of conodonts assigned to nine genera: *Carnepigondolella*, *Epigondolella*, *Kraussodontus,* *Metapolygnathus*, *Mockina*, *Neogondolella*, *Paragondolella*, *Parvigondolella*, *Primatella*, and *Quadralella.* The following six conodont zones were established based on the first occurrences (FO) and age ranges of diagnostic species in section N.

***Paragondolella*? *tadpole* interval Zone**

Definition.—The base of this zone is defined by the FO of the *Paragondolella*? *tadpole*. The top of this zone is defined by the FO of *Quadralella tuvalica.*

Stratotype and type horizons.—Sample NCL-185 to NCU-70 of section N.

Faunal character.—This zone is characterized by the FO of *Paragondolella*? *tadpole*, *Neogondolella* cf. *liardensis*, *P. auriformis P. inclinata* and *P. praelindae*.

***Quadralella tuvalica* interval Zone**

Definition.—The lower boundary of this zone is defined by the FO of the *Quadralella tuvalica.* The top of this zone is defined by the FO of *Epigondolella quadrata.*

Stratotype and type horizons.—Sample NCU-70 to N-H of section N.

Faunal character.—The fauna is characterized by FO of *Carnepigondolella* cf. *pseudodiebeli*, *C.* aff. *samueli*, *C. zoae*, *Kraussodontus ludingtonensis*, *K. roberti* alpha morphotype, *Metapolygnathus* cf. *communisti*, *Primatella orchardi*, *Quadralella postlobata*, *Q. carpathica*, *Quadralella noah*, *Q. tuvalica* and *Q.* sp. indet. A. The taxonomic diversity is high (12 species were determined).

Epigondolella quadrata interval Zone

Definition.—The base of this zone is defined by the FO of *Epigondolella quadrata*. The top of this zone is defined by the FO of *E. triangularis*.

Stratotype and type horizons.—Sample N-H to NHC-13 of section N.

Faunal character.—The FOs of *Epigondolella spatulata* and *E. quadrata* are recorded during this interval.

Epigondolella triangularis interval Zone

Definition.—The lower boundary of this zone is defined by the FO of *Epigondolella triangularis*, and the upper boundary by the FO of *Mockina postera*.

Stratotype and type horizons.—NHC-13 to NHC-15 of section N.

Faunal character.—Fauna is characterized by the continuous occurrence of *Epigondolella quadrata* and the FOs of *E. triangularis* and *E. rigoi*.

Mockina postera interval Zone

Definition.—The base of this zone is marked by the FO of *Mockina postera*. The top of this zone is defined by the FO of *M. bidentata*.

Stratotype and type horizons.—Sample NHC-15 to NHR-45 of section N.

Faunal character.—Fauna is characterized by the FOs of and *Mockina postera* and *M. spiculata*. The continuous occurrences of *Epigondolella quadrata* beta morphotype and *E. triangularis* are recorded in this interval.

***Mockina bidentata* Zone**

Definition.—The FO of *Mockina bidentata* defines the base of this zone. The top of this zone is not defined.

Stratotype and type horizons.—Sample NHR-45 to the top of section N.

Faunal character.—The accompanied fauna includes *Mockina bidentata*, *M. elongata*, *M. mosheri* morphotype A, *M. mosheri* morphotype B, *M. slovakensis*, *M. spiculata*, *M.* aff. *zapfei*, *Mockina* sp. indet. A, *Mockina* sp. indet. B, *Parvigondolella andrusovi* and *P.* aff. *vrielyncki*. The taxonomic diversity is high (11 species were determined).

Discussion

Conodont biostratigraphic correlations with other areas

The Upper Triassic conodont fauna of sections N and Q yields several common species that can be biostratigraphically correlated with sections in British Columbia, Sicily, and the

Chichibu and Tamba belts of Japan (Figures 5, 6). Of these, the Black Bear Ridge section in British Columbia and the Pizzo Mondello section in Sicily are of particular importance because these sections are GSSP candidate sections containing the Carnian-Norian boundary. The bioevents in sections N and Q are recognized (upwardly) as the first occurrences of *Paragondolella*? *tadpole*, *Quadralella tuvalica*, *Epigondolella quadrata*, *E. triangularis*, *Mockina postera*, and *M. bidentata*. This stratigraphic order is consistent with the order of these species in British Columbia (Orchard, 1991a, b, 2007a, 2014; Orchard *et al*., 2001), the Pizzo Mondello section (Mazza *et al*., 2012b) and other sections in Japan (Koike, 1981; Ishida and Hirsch, 2001; Mikami *et al*., 2008). Based on this comparison, we replaced the original names with the recent taxonomic names, where necessary, to avoid notational discrepancies.

The *Paragondolella*? *tadpole* interval Zone in our study correlates with the lower Carnian *Metapolygnathus tadpole* Zone in British Columbia (Orchard, 2007a) based on the abundant *Neogondolella liardensis* and common *P.*? *tadpole* in the latter. The *P.*? *tadpole* Zone can then be correlated with the ammonoid *Desatoyense* Zone through the *Obesum* Zone to the *Nanseni* Zone, based on the direct correlation of the conodonts and ammonoids in the same section in British Columbia (Orchard, 2007a). The co-occurrence of *P.*? *tadpole* and *Q. polygnathiformis* has also been reported in the Carnian successions in the Salzkammergut area, Austria, and designated the 'tadpole Interval Zone' (Hornung, 2006).

The *Quadralella tuvalica* interval Zone is equivalent to the interval ranging from the upper-Carnian *Carnepigondolella samueli* Zone to the *Acuminatella acuminata–Parapetella prominens* Subzone in British Columbia (Carter and Orchard, 2013; Orchard, 2014). The

assigned age is inferred from its direct correlation with the ammonoid *Welleri* Zone to the *Macrolobatus* Zone of Orchard (2014). Although the biostratigraphy at the Pizzo Mondello section is illustrated in the figures of Mazza *et al*. (2012b) without any designation of the conodont biozones, our *Q. tuvalica* Zone is assignable to the stratigraphic interval from NA0 to PM20 (see figure 2 of Mazza *et al*., 2012b) by the occurrence of *Q. tuvalica*. The *Neogondolella nodosa* Zone in the Taho, Kamura, and Oze sections (Koike, 1981) probably also corresponds to the *Q. tuvalica* interval Zone., because *Q. tuvalica* seems to be included in *N. nodosa*, which occur in these sections, based on a recent taxonomic analysis of the illustrated specimens. Although *Q. nodosa* was regarded as a possible lower Carnian species (Kozur *et al.*, 2009), the age and taxonomy of this species remains under debate (e.g. Kili., *et al.*, 2015). The co-occurrence of conodonts and radiolarians in British Columbia suggests that the radiolarian fauna of Assemblages 2c and 3 (Carter and Orchard, 2013) also correlate with this interval zone.

The *Epigondolella quadrata* interval Zone in our study is comparable to the stratigraphic interval from NA42 to PM43 (see figure 2 of Mazza *et al*., 2012b) based on the co-occurrence of *E. quadrata* and *E. spatulata*, and the first occurrence of *E. triangularis*. Mazza *et al*. (2012b) distinguished two morphotypes of *E. quadrata*: an intermediate form and an advanced form. The advanced form of *E. quadrata* is stratigraphically younger than the intermediate form and does not co-occur with *E. spatulata*. The *E. quadrata* obtained from section N is regarded as the intermediate form based on its morphology and its co-occurrence with *E. spatulata*. Orchard (2014) suggested a probable correlation between the basal *E. quadrata* Zone at Black Bear Ridge and the stratigraphic level of the first occurrence of the *E. quadrata* advanced form

(sample NA58) at the Pizzo Mondello section of Mazza *et al.* (2012b); consequently, the base of our *E. quadrata* interval Zone is below the base of the *E. quadrata* Zone of Orchard (2014). The *E. quadrata* Zone of Orchard (2014) at the Black Bear Ridge section and the representative species are dated as early Norian by their association with the ammonoid upper *Kerri* Zone to lower *Dawsoni* Zone (Orchard, 1991b, 2014; Orchard *et al*., 2001). We also note that the *E. quadrata* Zone of Orchard (1991b, 2014) correlates directly with radiolarian Assemblage 6 of Carter and Orchard (2013). The first occurrence datum of *E. quadrata* in Japan correlates with a lower Norian level based on these correlations and co-occurrence with *E. spatulata* in Section N. The conodont zone that correlates with our *E. quadrata* Zone in Japan is known as the *quadrata-spatulata* Zone in the Jifukudani section (Mikami *et al*., 2008) and the *E. spatulata* Zone in the Taho, Kamura, and Oze sections (Koike, 1981), according to a recent taxonomic analysis of the illustrated specimens.

The *Epigondolella triangularis* interval Zone is equivalent to the lower-Norian Middle to Upper *E. triangularis* Zone sensu Orchard (1991b), based on the occurrence of *E. triangularis triangularis* (*E. triangularis* in this paper). The *E. triangularis* Zone of Orchard (1991b) correlates well with part of the *Dawsoni* ammonoid Zone and the entire *Magnus* ammonoid Zone in the Black Bear Ridge section, indicating the lower Norian (Orchard, 1991a, b, 2014; Orchard *et al*., 2001). Carter and Orchard (2013) noted the co-occurrence of *E.* ex. gr. *triangularis* with their defined radiolarian Assemblage 7 in Haida Gwaii section.

The *Mockina postera* interval Zone correlates with the middle-Norian *E. postera* Zone of Orchard (1991a), which was dated by the associated ammonoids, indicative of the *Columbianus*

Subzone II ammonoid Zone in British Columbia (Orchard, 1991a, b; Orchard *et al*., 2001). The *M. postera* interval Zone also correlates with the *postera* Zone at the Hisaidani section (Ishida and Hirsch, 2001) and the *multidentata* zone at Kamura, Taho, and Oze (Koike, 1981), based on the occurrence of *M. postera*.

The *Mockina bidentata* Zone is equivalent to the *E. bidentata* Zone sensu Orchard (1991a) in British Columbia (Orchard, 1991a, b; Orchard *et al.*, 2001). According to the occurrence of *M. bidentata* in our studied sections, the interval from sample PM109 to NR1 in the Pizzo Mondello section (see figure 3 of Mazza *et al.*, 2012b) and the *bidentata* Zone at Kamura, Taho, and Oze (Koike, 1981) also correspond to this conodont zone. Orchard's *E. bidentata* Zone correlates directly with the ammonoid *Columbianus* Subzone IV and *Cordilleranus* Zone in British Columbia (Orchard *et al*., 2001), suggesting the late Norian. This zone also correlates with the radiolarian *Deweveri* Zone in Haida Gwaii in Canada (Carter and Orchard, 2007).

In the conodont fauna of the study section, *Mockina slovakensis*, *M. zapfei*, *Paragondolella praelindae* and *P. auriformis* are only reported from Tethyan regions, whereas the occurrences of *Kraussodontus ludingtonensis*, *K. roberti*, *M. mosheri*, *Neogondolella liardensis*, *Quadralella postlobata* are only known from North America. Especially, *K. ludingtonensis* and *K. roberti*, reported as new taxa from British Columbia (Orchard, 2014), have not been reported elsewhere yet. These results suggest that the conodont taxa from the study section in Japan may provide an important faunal link between Tethys and North American regions, as other paleobiogeographic studies have shown (Klets, 2005; Klets and Kopylova, 2008).

Carnian-Norian boundary interval in section N

A significant conodont faunal turnover and a negative organic carbon isotope excursion have been reported near the Carnian-Norian boundary in the GSSP candidate sections for the basal Norian (e.g. Zonneveld *et al*., 2010). To establish high-resolution correlations and to understand the timing of the faunal turnovers in different sections, it was necessary to constrain the Carnian-Norian boundary interval in our study section based on the conodont biostratigraphy. However, the conodont-based correlation with the GSSP candidate sections for the Carnian-Norian boundary at Black Bear Ridge and Pizzo Mondello is difficult because of the difference of conodont faunas and taxonomic approaches (Orchard, 2014).

Mazza *et al*. (2010) recognized three major turnovers of conodont genera near the Carnian-Norian boundary in the Pizzo Mondello section: T1, T2, and T3. Here, to constrain the Carnian-Norian boundary interval in section N, we discuss (1) the identification of these faunal turnovers in section N; and (2) the relationship between these faunal events and the Carnian-Norian boundary interval.

Turnovers 1, 2, and 3 (T1, T2, and T3).—T1 is marked by the disappearance of almost all *Carnepigondolella* and their replacement by *Epigondolella*, followed by the disappearance of *Paragondolella*. This bioevent is not clearly identifiable in either Black Bear Ridge (Orchard, 2014) or section N because *Epigondolella* occurs much earlier at Pizzo Mondello than at Black Bear Ridge or in section N.

In T2, *Epigondolella* suddenly decreases and *Metapolygnathus* becomes dominant. This event has been interpreted as the event in which *Primatella* spp., *Quadralella praecommunisti*, *Kraussodontus*, and *Parapetella* become dominant, and correlates approximately with the *samueli–primitia* zonal boundary in British Columbia (Orchard, 2014). This turnover is not identified at section N because these species are rare.

T3 is characterized by the disappearance of most *Metapolygnathus* and their replacement by 'advanced' *Epigondolella* and *Norigondolella*. Orchard (2014) regarded the 'advanced' *Epigondolella* referred to by Mazza *et al*. (2012b) as *Primatella* species, and correlated level T3 with a position close to the base of the *asymmetrica-Norigondolella* Subzone of the *primitia* Zone. This level is approximately comparable to the *Quadralella tuvalica-E. quadrata* zonal boundary in section N, based on the occurrence of *Epigondolella* species in the basal *E. quadrata* interval Zone.

Carnian-Norian boundary interval.—Three conodont bioevents were identified between T2 and T3 and are bounded by the 'Carnian-Norian boundary interval' in Pizzo Mondello (Mazza *et al*. 2012b). These bioevents were reinterpreted by Orchard (2014) based on his new nomenclatural definition, and characterized by the first occurrence of *Metapolygnathus parvus*, *Parapetella destinae* (= *Metapolygnathus echinatus* sensu Orchard), and *Primatella gulloae* (= *Carnepigondolella gulloae*). All of these events are included in the *parvus* Subzone (between beds 18 and 20) at Black Bear Ridge (Orchard, 2014). The Carnian-Norian boundary interval in the Black Bear Ridge section begins below the base of the *parvus* Subzone and continues up to near the base of the *asymmetrica-Norigondolella* Subzone of the *primitia* Zone (Orchard, 2014;

Onoue *et al*., 2016b). In short, in the Carnian-Norian boundary interval in the Pizzo Mondello section and the Black Bear Ridge section, many diminutive elements, including *M. parvus*, become dominant. However, these elements are absent from section N. which may be explained by short hiatuses in the bedded chert succession of section N, or the low distribution density of these elements or most of the diminutive taxa except for *M. parvus* and *M. echinatus* may be endemic species in North America. Onoue *et al*. (2012) estimated the sedimentation rate of the Late Triassic pelagic bedded cherts to be ca. 1 mm/ky. According to Muttoni *et al*. (2001, 2004), the Scillato Formation in Pizzo Mondello is characterized by a high sedimentation rate (20–30 m/my) compared with the classic Tethyan section. The Carnian-Norian boundary interval is restricted to ~3.5 m of the bedded limestone succession at Black Bear Ridge and ~12 m of the bedded cherty limestone at Pizzo Mondello, and the boundary interval in the bedded chert succession may be restricted to a narrower interval in section N (less than 60 cm) than in those two sections. Therefore, the conodont turnover events at the Carnian-Norian boundary interval are thought to be included in the stratigraphic interval between the last occurrence of Carnian species and the first occurrence of Norian species in section N (from samples N-130 to N-H). Further high-resolution sampling and quantitative assemblage data are required to refine the positions of these bioevents.

Correlation between conodont and radiolarian biostratigraphies

We established six conodont zones based on the first occurrences of the representative conodont species of each zone in the lower Carnian (Julian) to upper Norian (Sevatian) intervals

in Sugiyama's N and Q sections. In chronological order, these are the *Paragondolella*? *tadpole*, *Quadralella tuvalica*, *Epigondolella quadrata*, *E. triangularis*, *Mockina postera*, and *M. bidentata* zones. The lithostratigraphic intervals examined in the present study cover the stratotypes of Sugiyama's radiolarian TR5B Zone in section Q, and the TR6A and TR6B zones in section N (Figures 3, 4). The upper part of section N in our study correlates with radiolarian TR7 to TR8A, although this section is not defined as the stratotype of these radiolarian zones (Figure 4). The conodont biozones established in the present study can then be correlated with Sugiyama's (1997) six radiolarian zones.

Carnian.—Sugiyama (1997) correlated the interval from the upper part of TR4B to the lower part of TR6A with the Carnian. The interval of section Q examined in the present study starts somewhere in TR5A, which is defined by the first appearance of the genus *Capnuchosphaera*. Nakada *et al.* (2014) examined the radiolarian biostratigraphy of Sugiyama's section R and placed the lower and upper Carnian boundary in the upper part of TR5A. The lower and upper Carnian are locally designated 'Julian' and 'Tuvalian', respectively, and are determined by the boundary between the conodont *Paragondolella*? *tadpole* and *Q. polygnathiformis* zones (Ogg, 2012). The boundary between the *P.*? *tadpole* and *Q. polygnathiformis* zones is not detectable in sections N or Q because *Q. polygnathiformis* does not occur in either. Instead, we tentatively placed the lower-upper Carnian boundary between the *P.*? *tadpole* and *Q. tuvalica* zones in section N (between samples NCU24 to N-D), which lies around the radiolarian TR5A-TR5B boundary. This correlation supports the results of Nakada *et al*. (2014).

Carnian-Norian boundary.—The potential GSSP Carnian-Norian boundary is tentatively placed between the *Quadralella tuvalica* and *Epigondolella quadrata* interval Zones. The base of the *E. quadrata* interval Zone is found in both sections N and Q, where the first occurrence of *E. quadrata* occurs around the boundary between the radiolarian TR5B and TR6A zones, suggesting the probable Carnian-Norian boundary. Because Sugiyama (1997) presumed the Carnian–Norian boundary to lie within TR6A, our results refine the correlation between the geological timescale and the radiolarian biozones. The base of TR6A is defined by the first occurrence of the genus *Capnodoce*. The first occurrence of the genus *Capnodoce* seems not to be a marker for the base of the Norian, because the first *Capnodoce* species (*C. antigua* and *C. gracilis*) occur in the latest Carnian 'lower *primita*' conodont zone from Haida Gwaii (Carter and Orchard, 2013). The base of the TR6A is slightly older than the base of the *E. quadrata* interval Zone (Figure 3), which is consistent with the interpretation that the Carnian-Norian boundary is situated near the boundary between the *Quadralella tuvalica* and *Epigondolella quadrata* interval Zones.

Ikeda and Tada (2014) examined Sugiyama's sections and then lowered the Carnian-Norian boundary to TR5B, based on the occurrences of *Capnuchosphaera lea*, *Capnuchosphaera triassica*, and *Capnuchosphaera deweveri*. According to Ikeda and Tada (2014), *Capnuchosphaera lea* ranged across the Carnian-Norian boundary at the Pizzo Mondello section, which is the candidate section for the base of the GSSP Norian (Nicora *et al.*, 2007; Mazza *et al.*, 2010, 2012b). The direct correlation between the conodont and radiolarian

biostratigraphies in our study inevitably assigns the Carnian-Norian boundary to the basal part of TR6A.

Norian.—The Norian is subdivided into three substages in the Tethys: the Lacian, Alaunian, and Sevatian. The boundary between the conodont *Epigondolella triangularis* and *E. postera* zones sensu Orchard (1991b) is regarded as the lower-middle Norian boundary based on the conodont biostratigraphy (Orchard, 1991a, b). In our study, this boundary lies within the radiolarian TR6A Zone, whose base is defined by the first occurrence of the genus *Trialatus*. The lowermost part of the conodont *M. postera* interval Zone is marked by the first occurrences of radiolaria *Capnodoce sarisa* and *Xiphosphaera fistulata*. These radiolarians have potential utility in specifying the position of the Lacian-Alaunian boundary.

The Alaunian-Sevatian boundary is interesting for its relationship to significant turnovers of radiolarians and conodonts, but its identification is somewhat problematic. In this boundary interval, *Epigondolella quadrata*, *E. triangularis* and *Mockina. postera* disappeared, and *E.* sp. indet. B, *E. elongata*, *Mockina bidentata*, *M. mosheri* morphotype A and *Parvigondolella* aff. *vrielyncki* appeared. This conodont faunal turnover in the boundary interval between the conodont *Mockina postera* interval Zone and the *M. bidentata* Zone is coincident with a radiolarian faunal turnover event (Onoue *et al.*, 2016a) in the boundary interval between the radiolarian zones TR6A and TR6B. TR6B is defined by the last occurrence of *Trialatus robustus*. The *M. bidentata* Zone correlates directly with Sugiyama's TR6B, TR7, and a large part of TR8A. The correlation between the top of the *M. bidentata* Zone and the top of TR8A is unclear in our study section. The first occurrence of *M. bidentata* is considered to define the

Alaunian-Sevatian boundary (Channell *et al*., 2003; Rigo *et al*, 2005, 2012; Krystyn, 2008; Mazza *et al*., 2012b). Rigo *et al*. (2016 and references therein) correlated the base of the *M. bidentata* Zone with the North America ammonoid *Gnomohalorites cordilleranus* or Tethyan *Sagenites quinquepuctaus* Zone, a Sevatian zone. This opinion was shared by Uno *et al*. (2015), who regarded the first occurrence horizon of *M. bidentata* as the base of the upper Norian in Sugiyama's section N. However, several different opinions about the Alaunian–Sevatian boundary have been proposed. The first appearance of *M. bidentata* in the Hallstatt region is approximately in the middle part of the *Columbianus* ammonoid Zone (Krystyn, 1980), an Alaunian zone. This conodont species also occurs in the *Columbianus* Subzone IV ammonoid Zone in British Columbia (Orchard *et al*., 2001). Moreover, Onoue *et al.* (2012, 2016a) demonstrated that the lower part of the *M. bidentata* Zone in Sugiyama's section N is marked by the radiolarian fauna of the TR6B, which is assigned to the Alaunian. Since the Alaunian radiolarian fauna disappeared within radiolarian biozone 6B, Onoue *et al.* (2016a) correlated the radiolarian zonal boundary between TR6B and TR7 with the Alaunian-Sevatian boundary. Our comprehensive examination of the occurrences of conodonts and radiolarians indicates that the boundary between the *M. postera* and *M. bidentata* zones might not coincide with the Alaunian-Sevatian boundary, at least in Sugiyama's section N.

Conclusions

1) Based on recent conodont taxonomy, new conodont biostratigraphic data are presented from the lower Carnian to the upper Norian bedded chert succession in central Japan, where the standard radiolarian biostratigraphy has previously been investigated (Sugiyama, 1997).

2) Based on the stratigraphic distribution of marker species, six conodont zones were defined: *Paragondolella*? *tadpole* interval Zone, *Quadralella tuvalica* interval Zone, *Epigondolella quadrata* interval Zone, *E. triangularis* interval Zone, *Mockina postera* interval Zone, and *M. bidentata* Zone. These were correlated with the coeval radiolarian zonation established by Sugiyama (1997).

3) The defined conodont zonation of section N is comparable to that in British Columbia (Orchard, 1991a, b, 2007a, 2014; Orchard *et al.*, 2001), the Pizzo Mondello section (Mazza *et al*., 2012b), and other sections in southwest Japan (Koike, 1981; Ishida and Hirsch, 2001; Mikami *et al*., 2008).

4) The Carnian-Norian boundary interval in section N is tentatively placed between the last occurrence of Carnian species and the first occurrence of Norian species (from sample N-130 to sample N-H in section N) because of the absence of *Metapolygnathus parvus* and other diminutive elements reported from the GSSP candidate sections for the Carnian-Norian boundary.

Systematic description

All illustrated material is stored at the Faculty of Science, Kumamoto University (Institution abbreviation: KMSP = Registry number of the Faculty of Science, Kumamoto University). All descriptions are based on disarticulated P_1 elements.

Class Conodonta Eichenberg, 1930

Order Ozarkodinida Dzik, 1976

Superfamily Gondolelloidea (Lindström, 1970)

Family Gondolellidea Lindström, 1970

Genus ***Carnepigondolella*** Kozur, 2003

Type species.—*Metapolygnathus zoae* Orchard, 1991b.

Carnepigondolella aff. ***samueli*** (Orchard, 1991b) beta morphotype

Figure 7.1

aff. *Carnepigondolella samueli* (Orchard), Orchard, 2007b, figs. 1.22-1.24; Nicora *et al*., 2007, pl. 1, fig. 5; Balini *et al*., 2010, pl. 2, fig. 13; Mazza *et al*., 2012b, p. 98, 100, pl. 3, fig. 1 (only).

Carnepigondolella samueli (Orchard) beta morphotype, Orchard, 2014, p. 51, 53, figs. 39.13–39.18.

Material examined.—One specimen, KMSP-100001, from N-130.

Description.—One broken rectangular gondola-like P_1 element, characterized by rectangular platform which bears more than 6 small, sharp and discrete nodes on each lateral margin. Surface of platform margin is covered by microreticulation. The posterior platform is rounded and laterally expanded. This expansion is asymmetric. A groove runs from basal pit to anterior end; rounded basal pit surrounded by basal cavity with an outline similar to the outline of the platform margin; end of the cavity is bifurcated. The pit lies near the posterior end of the keel.

Remarks.—Two morphotype of this species were distinguished in Black Bear Ridge section and the holotype of this species was regarded as alpha morphotype by Orchard (2014). An alpha morphotype has a rectangular platform, while a beta morphotype has a larger, asymmetrical platform with inner postero-lateral margin, which is laterally expanded. The described element is similar to *Carnepigondolella samueli* beta morphotype but differ in having a straight longitudinal axis and a more rounded posterior platform.

Carnepigondolella zoae (Orchard, 1991b)

Figures 7.2, 7.3

Metapolygnathus sp. F Orchard, 1991a, p. 176, pl. 1, figs. 7–11, pl. 3, fig. B.

Metapolygnathus zoae Orchard, 1991b, p. 319, pl. 1, figs. 7–9.

Paragondolella carpathica (Mock), Channell *et al*., 2003, pl. A1, fig. 7.

Epigondolella nodosa nodosa (Hayashi), Channell *et al*., 2003, pl. A1, fig. 37.

Epigondolella nodosa zoae (Orchard), Channell *et al*., 2003, pl. A1, fig. 16, 34, 39.

Carnepigondolella zoae (Orchard), Mazza *et al.*, 2010, pl. I, fig. 7; Balini *et al*., 2010, pl. 2, fig. 7; Orchard, 2014, p. 54, figs. 35.7–35.15.

Carnepigondolella zoae B (Orchard), Mazza *et al.*, 2010, pl. I, fig. 8.

Carnepigondolella zoae (Orchard) central morphotype, Mazza *et al*., 2012b, p. 103, pl. 4, fig. 1 (only).

Material examined.—Two specimens, KMSP-100002, from QU1-170 and KMSP-100003, from N-115.

Description.—The P_1 elements have elongate subrectangular platform with a length-to-breadth ratio lying between 2:1 and 2.5:1. The platform bears 3-4 rounded nodes on the lateral platform margin and a distinct constriction in the posterior one-third. The blade, about one-third total element length, passes onto the platform as 4-5 carinal nodes. The pit, located posterior half of the platform, slightly shifted anteriorly within the keel.

Remarks.—The described specimens are similar to the holotype (Orchard, 1991b, pl. 1, figs. 7-9) and *Carnepigondolella zoae* central morphotype (Mazza *et al*., 2012b, pl. 4, fig. 1) in having 3-4 rounded nodes on the lateral platform margin and a distinct constriction in the posterior one-third. Mazza *et al*. (2012b) also recognized Morphotype A and B, but these morphotype differ from our specimens in lacking a distinct platform constriction.

Genus ***Epigondolella*** Mosher, 1968a

Type species. —*Polygnathus abneptis* Huckriede, 1958

Epigondolella quadrata Orchard, 1991b, beta morphotype

Figures 7.4, 7.5

Epigondolella abneptis (Huckriede), Koike, 1981, p. 51, pl. 2, figs. 26, 27 (only) ; Channell *et al*., 2003, pl. A2, fig. 36, pl. A3, 18 (only).

Epigondolella abneptis subsp. A population, Orchard, 1983, p. 179, fig. 15.F (only).

Epigondolella quadrata Orchard, 1991b, p. 311, pl. 2, figs. 7–9 (only); Nicora *et al*., 2007, pl. 3, figs. 8, 9; Mazza *et al*., 2010, pl. II, figs. 2, 3, pl. III, fig. 8; Mazza *et al.*, 2012b, p. 106, pl. 5, figs. 2, 4–10 (only); Carter and Orchard, 2013, figs. 7.22–7.24.

Ancyrogondolella quadrata (Orchard), Ishida and Hirsch, 2001, p. 236, pl. 2, figs. 5, 6, 8 (non figs. 4, 7); Mikami *et al*., 2008, p. 174, pl. 2, fig. 6 (non figs. 1–5), pl. 3, figs. 4, (non fig. 5); Ishida *et al*., 2015, p. 11, pl. 1, figs. 10, 11, pl. 2, figs. 3, 4.

Epigondolella quadrata Orchard, beta morphotype, Orchard, 2014, p. 55–57, figs. 40.19–40.27.

Material examined.—Two specimens, KMSP-100004, from QU2-346 and KMSP-100005, from QU2-221.

Description.—The P_1 elements have a subrectangular posterior platform margin with no ornamentation except for microreticulation, and 2-3 sharp denticles on the anterior platform margin. The posteriormost denticle is the highest and double the height of the platform. The blade is between 1/3 and 1/2 total element length and composed of 5–6 denticles forming convex upper profile. The pit is submedial under the platform and slightly shifted anteriorly within the keel, which has a bifurcated or squared-off termination.

Remarks.—Orchard (1983) distinguished two *Epigondolella abneptis* groups based on the morphology of the posterior platform, namely *E. abneptis* subsp. A population and B population. *E. quadrata* was differentiated from *E. abneptis* subsp. A population by Orchard (1991b). Moreover, two morphotypes were distinguished by Orchard (2014) based on the posterior platform shapes. Alpha morphotype has an expanded posterior platform margin with acutely angled postero-lateral corners, while beta morphotype has a subrectangular posterior platform with subparallel lateral margins. A shape of the posterior platform of our specimens is similar to that of beta morphotype of Orchard (2014).

Epigondolella rigoi Kozur, 2007

Figure 7.6

Epigondolella spatulata (Hayashi), Koike, 1981, pl. 2, figs. 35, 36 (only); Orchard, 1991b, p. 312, pl. 2, figs. 4–6, 11; Muttoni *et al.*, 2001, fig. 10.9.

Epigondolella abneptis subsp. A population Orchard, 1983, p. 179, fig. 4B (only).

Epigondolella quadrata (Orchard), Martini *et al*., 2000, pl. V, figs. 3, 4.

Metapolygnathus abneptis spatulatus (Hayashi), Noyan and Vrielynck, 2000, p. 590-591, figs. 8.2-8.5 (only).

Ancyrogondolella spatulata (Hayashi), Ishida and Hirsch, 2001, p. 236, pl. 3, figs. 5–7, pl. 4, figs. 1, 3, 5; Mikami *et al*., 2008, pl. 2, fig. 7 (only); Ishida *et al.*, 2015, p. 11, pl. 1, fig. 12.

Epigondolella abneptis (Huckriede), Channell *et al*., 2003, pl. A1, figs. 27, 30, 33.

Epigondolella rigoi Kozur, in Noyan and Kozur, 2007, p. 167, figs. 6.2–6.5; Nicora *et al*., 2007, pl. 3, fig. 12, pl. 4, fig. 6., Mazza *et al*., 2010, pl. II, fig. 5; Balini *et al*., 2010, pl. 3, fig. 8, Mazza *et al*., 2012b, p. 108, pl. 6, figs. 1–7.

Material examined.—One specimen, KMSP-100006, from NCU-430.

Description.—The P_1 element is characterized by a subtriangular platform, which is 2/3 total element length. The anterior platform margin bears 2–3 high denticles, and the laterally widened posterior platform is inornate or weakly undulated. The short free blade is composed of 3–4 denticles and descends onto the platform as a row of 4–5 carinal nodes that terminate on the anterior platform. The cusp is the penultimate denticle of the carina and followed by a large accessory node. The pit is submedial under the platform, and subterminal within the keel, which has a bifurcated end.

Remarks.—Sub-triangular platform of the *Epigondolella rigoi* is similar to that of *E. triangularis*, but differ in lacking denticles on the posterior platform margin. *E. quadrata* also

resembles *E. rigoi*, but *E. quadrata* does not have a laterally strongly expanded posterior platform.

Epigondolella spatulata (Hayashi, 1968)

Figure 7.9

Gladigondolella abneptis var. *spatulata* Hayashi, 1968, p. 69, pl. 2, fig. 5.

Epigondolella abneptis (Huckriede), Cafiero and Bonardi, 1981, pl. 58, fig. 10.

Ancyrogondolella spatulata (Hayashi), Mikami *et al*., 2008, p. 174, pl. 2, fig. 12, (non figs. 7-10), pl. 3, figs. 6–8.

Epigondolella spatulata (Hayashi), Mazza *et al*., 2010, pl. III, figs. 5, 6; Balini *et al*., 2010, pl. 4, fig. 6; Mazza *et al*., 2012b, p. 110, pl. 6, fig. 8.

Material examined.—One specimen, KMSP-100009, from N-H.

Description.—The P_1 element is characterized by broad oval platform with an ornamented margin and a reduced anterior trough margin. 2–3 denticles occur on the lateral platform margin. The posterior platform may have additional nodes that are apart from continuation of the carinal nodes, and posterior platform margin is weakly ridged. The blade is about 1/2 total element length and composed of 5 denticles. The terminal cusp of the carina is submedial in position with respect to the platform. The pit lies beneath the platform midlength or slightly shifted anteriorly within the keel, which is commonly bifurcated.

Remarks.—*Epigondolella rigoi* is similar to this species, but differ in having a sub-triangular platform.

Epigondolella triangularis (Budurov, 1972)

Figure 7.7

Ancyrogondolella triangularis Budurov, 1972, p. 857, pl. 1, figs. 3–6; Buryi, 1997, pl. II, figs. 16, 17; Ishida and Hirsch, 2001, p. 234, 236, pl. 2, fig. 3.

Epigondolella abneptis spatulata (Hayashi), Krystyn, 1980, pl. 13, fig. 14 (only).

Epigondolella abneptis (Huckriede), Cafiero and Bonardi, 1981, pl. 58, fig. 9 (only).

Epigondolella abneptis subsp. B (Huckriede), Orchard, 1983, p. 181, fig. 6A, E, L, Q (only).

Epigondolella triangularis (Budurov), Orchard, 1991a, pl. 4, fig. 12; Nicoll and Foster, 1994, p. 109, figs. 8.1–8.3, Martini *et al*., 2000, pl. V, figs. 5–6 (only); Channell *et al*., 2003, pl. A3, figs. 88 (only); Mazza *et al*., 2010, pl. III, fig. 9; Balini *et al*., 2010, pl. 4, fig. 7.

Epigondolella triangularis (Budurov) *sensu lato*, Orchard, 1991b, p. 314, pl. 3, figs. 4–6.

Metapolygnathus spatulata (Hayashi), Buryi, 1996, pl. 1, fig. 1.

Material examined.—One specimen, KMSP-100007, from NCU-430.

Description.—The P1 element is characterized by a sub-triangular, ornate platform with a lateral expansion in the posterior platform. The anterior platform margins are ornamented with 3–4 sharp, prominent denticles, and outer posterior margin bear several sharp, lower nodes that

often project beyond the platform margin giving the posterior platform a serrated outline. The blade composed of 7–9 denticles is about 1/3 of the total element length, and descends onto the platform as discrete, round carinal nodes. The lower surface has a pit located in a submedial position and a bifurcated keel, which extends to the posterolateral corners.

Remarks.—*E. rigoi* also has a sub-triangular platform, but differ in lacking ornamentation on the posterior platform margin. Although *E. spatulata* has an ornamented posterior platform margin, the posterior platform shape is subcircular.

Genus ***Kraussodontus*** Orchard, 2013

Type species.—*Kraussodontus peteri* Orchard, 2013

Kraussodontus ludingtonensis Orchard, 2014

Figure 7.8

Kraussodontus ludingtonensis Orchard, 2014, p. 59, figs. 42.1–42.11.

Material examined.—One specimen, KMSP-100008, from N-117.

Description.—The P_1 element has a short blade and an elongate ovoid platform with a rounded and upturned posterior platform margin, a length-to-breadth ratio of between 2.5:1 and 3:1, and subparallel lateral margin. All platform margins are inornate except for

microreticulation. In profile, the element is arched and the blade is relatively low, composed of about five denticles and continues as a low carina. Lower surface bears a narrow basal keel and a pit located beneath the posterior platform.

Remarks.—The described specimen is characterized by a short, low blade and rounded posterior platform margin. These distinctive features enable it to be assigned with reasonable confidence to this species.

Kraussodontus roberti Orchard, 2014, alpha morphotype

Figures 8.1–8.3

Kraussodontus roberti Orchard alpha morphotype, 2014, figs. 43.23–43.40.

Material examined.—Three specimens, KMSP-100010, from N-121, KMSP-100011, from NCU-70 and KMSP-100012, from QU1-88.

Description.—The P_1 elements are characterized by long platform with a length-to-breadth ratio ranging from 1.5:1 to 2:1, a ovoid posterior platform margin and subparallel lateral platform margin. All platform margins have no ornamentation except for microreticulation. The blade is about 1/3 total element length and composed of highly fused denticles. The anterior platform margin may be slightly stepped. In profile, the elements are arched in the posterior third. The pit is located posterior of the platform midlength and anteriorly shifted in the keel, which commonly has a rounded termination.

Remarks.—Orchard (2014) differentiated two morphotype of this species, namely alpha morphotype and beta morphotype. Alpha morphotype has a longer platform and shorter blade than beta morphotype. The pit is situated under the center of the platform in the beta morphotype, while the alpha morphotype displays some variation in pit position. The described specimens have a relatively long platform and a pit located posterior of the platform midlength. These features enable us to distinguish the alpha morphotype.

Genus ***Mockina*** Kozur and Mostler, 1971

Type species.—*Tardogondolella abneptis postera* Kozur and Mostler, 1971

Mockina bidentata (Mosher, 1968a)

Figures 8.4, 8.5

Polygnathus abneptis Huckriede, 1958, p. 156, 157, pl. 14, figs. 32, 58 (only).

Epigondolella bidentata Mosher, 1968a, p. 936, pl. 118, figs. 31–35 (only); Mosher, 1968b, pl. 120, fig. 29–33 (only); Sweet *et al*., 1971, pl. 1, fig. 30; Kozur and Mock, 1972, pl. 1, figs. 15, 16 (only); Kozur and Mostler, 1972, pl. 4, figs. 3-5; Murata and Nagai, 1972, p. 716, pl. 9, figs. 21–24; Krystyn, 1973, pl. 5, fig. 7; Mosher, 1973, p. 160, pl. 18, figs. 23, 24, 28; Budurov, 1977, p. 45, pl. 1, fig. 7, pl. 2, fig. 4; Sweet in Ziegler, 1977, p. 157, Epigondolella-plate 1, fig. 6; Okami *et al*., 1978, pl. 1, figs. 5–9; Kolar, 1979, p. 314, pl. 1,

fig. 3, pl. 2, fig. 2; Isozaki and Matsuda, 1980, figs. 1, 2; Krystyn, 1980, pl. 14, figs. 1–3 (only); Cafiero and Bonardi, 1981, pl. 58, figs. 13–16; Koike, 1981, pl. 2, figs. 30, 31; Isozaki and Matsuda, 1982, p. 117, pl. 4, figs. 1–5; Orchard in Carter *et al*., 1989, pl. 1, fig. 13; Budurov and Sudar, 1990, pl. 5, figs. 9, 13–16; Orchard, 1991b, p. 307, pl. 4, fig. 12; Nicoll and Foster, 1994, p. 108, figs. 7.1, 7.2; Amodeo, 1999, pl. 1, figs. 20–22; Bertinelli *et al*., 2005, fig. 4.5; Rigo *et al*., 2005, fig. 4.6; Krystyn *et al*., 2007, pl. 1, figs. 5–14; Orchard *et al*., 2007b, figs. 7.18, 8.10, 8.11, 8.13, 8.17-8.20.

Tardogondolella bidentata (Mosher), Mock, 1971, pl. 4, fig. 3.

Metapolygnathus bidentatus (Mosher), Kozur, 1972, pl. 7, figs. 3–9, 15; Maejima and Matsuda, 1977, fig. 2.1; Gaździcki *et al*., 1979, pl. 5, figs. 10–12; Ishida, 1979, pl. 3, figs. 14, 15; Kovács and Kozur, 1980, pl. 15, fig. 1.

Epigondolella andrusovi (Kozur and Mock), Budurov, 1976, pl. 5, fig. 6; Budurov, 1977, p. 45, pl. 1, figs. 5, 6, pl. 2, figs. 3–5.

Epigondolella multidentata Mosher, Cafiero and Bonardi, 1981, pl. 58, fig. 17.

Epigondolella bidentata population, Orchard, 1983, p. 188, 189, figs. 15.W, 15.X (only).

Mockina bidentata (Mosher), Channell *et al*., 2003, pl. A2, figs. 44, 46–48, 51, 54; pl. A3, figs. 3, 4, 6, 7, 9, 27, 28, 37, 39, 41, 42, 47–51, 54, 56, 71, 72, 74–77, 79; Moix *et al*., 2007, pl. 2, fig. 3; Giordano *et al*., 2010, fig. 3.1 (only); Balini *et al*., 2010, pl. 4, fig. 9; Mazza *et al*., 2012b, p. 120, pl. 7, fig. 7; Rigo *et al*., 2016, fig. 3.3.

Material examined.—Two specimens, KMSP-100013, from NHR-45 and KMSP-100014, from NHR-70.

Description.—The P_1 elements are characterized by a short and narrow platform. The anterior platform margins bear a sharp denticle on each margin; a minor accessory denticle may appear on one side. The blade is about 1/2 element length and bears partly fused 5–6 denticles that descend onto the platform. The cusp is discrete in size and the pit lies beneath the center of platform.

Remarks.—As previous authors have already pointed out, this species can be easily confused with juvenile forms of the other middle and upper Norian species. *Mockina mosheri* has a longer posterior platform and more than 4 carinal nodes. *M. postera* and *M. englandi* have a broader platform. The short, narrow platform and a sharp denticle on each platform margin (specimen KMSP0004 has a minor accessory denticle on one side) of the described specimen are similar to those of the holotype (Mosher, 1968a, pl. 118, fig. 35) and specimens described by various authors (e.g. Orchard, 1991b; Mazza *et al*. 2012b).

Mockina elongata **(**Orchard, 1991b)

Figures 8.6, 8.7

Epigondolella postera (Kozur and Mostler) population, Orchard, 1983, p. 186–188, figs. 12.M, 12.N (only).

Epigondolella elongata Orchard, 1991b, p. 308, pl. 4, figs. 4–6, 15, 20, 21; Rigo *et al*., 2005, fig. 4.4.

Mockina cf. *elongata* (Orchard), Ishida and Hirsch, 2001, pl. 5, figs. 1, 2.

Material examined.—Two specimens, KMSP-100015, from NHR-42 and KMSP-100016, from NHR-56.

Description.—The platform is very slender with length-to-breath ratio of about 3:1 and slightly curved at the center of the platform. The keel also curved and posterior end of the keel is tapered. The anterior platform margins bear 1–2 denticles on the inner side and 2–3 on outer side, while the posterior platform has no ornamentation. The carinal nodes extend to the posterior end of the platform. The pit lies in the anterior half of the platform.

Remarks.—Orchard (1991b) differentiated this species from *Epigondolella postera* (Kozur and Mostler) population, which has broader and lobate posterior platform. The described specimen has an ellipsoid platform with 1-3 denticles (at least 2 denticles on one side) on each anterior platform margins and an anteriorly situated pit within the keel, which has a pointed termination. These distinctive features are shared with the type species (*Tardogondolella abneptis postera* Kozur and Mostler) of the genus *Mockina* and matches well with holotype of Orchard (1991b).

Mockina mosheri **(**Kozur and Mostler, 1971)

Figures 8.8–8.10

Epigondolella bidentata Mosher, 1968a, p. 936, pl. 118, fig. 36; Mosher, 1970, pl. 110, figs. 27, 28.

Tardogondolella mosheri Kozur and Mostler, 1971, p. 15.

Epigondolella ex gr. *bidentata* Mosher, Orchard, 1991a, pl. 4, fig. 22.

Epigondolella mosheri (Kozur and Mostler), Budurov, 1977, pl. 5, fig. 24, Orchard, 1991b, p. 309, 310, pl. 4, figs. 11, 13, 14; Carter and Orchard, 2007, pl. 2, figs. 1, 3–8, 10–13, 16–18; Orchard *et al*., 2007b, figs. 8.1-8.9.

Material examined.—Three specimens, KMSP-100017, from NHR-72, KMSP-100018, from QU3-163 and KMSP-100019, from QU3-163.

Description.—P_1 elements have a slender platform with a curved longitudinal axis. Each anterior platform margin bear a pair of denticles, and a minor accessory denticle may appear on one side. The posterior platform margin and the keel end are tapered. The pit lies anterior of the platform midlength.

Remarks.—The described elements are regarded as members of the genus *Mockina* (type species: *Tardogondolella abneptis postera* Kozur and Mostler), because these elements and type species share some features in the presence of a tapered platform with shape denticles, and an anteriorly situated pit within the keel, which has a pointed termination. These elements are similar to *Mockina bidentata* but differ in having a curved longitudinal axis, a broader platform and a minor accessory denticle.

Orchard (1994) distinguished morphotype A and B within the conodont collection obtained from the Pucará Group in Peru. Moreover, Orchard *et al*. (2007a) differentiated three morphotypes based on posterior platform ornament and reported Morphotype C from Gabbs Formation in New York Canyon.

Mockina mosheri **(**Kozur and Mostler, 1971) morphotype A

Figures 8.8, 8.9

Epigondolella mosheri (Kozur and Mostler), Orchard, 1991b, p. 309, pl. 4, figs. 11, 13, 14; Carter and Orchard, 2007, pl. 2, figs. 4, 6, 7, 11.

Epigondolella mosheri (Kozur and Mostler) Morphotype A, Orchard *et al*., 2007a, figs. 16, 17, 23–25.

Material examined.—Two specimens, KMSP-100017, from NHR-72 and KMSP-100018, from QU3-163.

Remarks.—Morphotype A is similar to the holotype and has a narrow and inornate anterior platform except for a small posterior node.

Mockina mosheri **(**Kozur and Mostler, 1971) morphotype B

Figures 8.10

Epigondolella mosheri (Kozur and Mostler) Morphotype B, Orchard, 1994, p. 207, pl. 1, figs. 1–9, 12; Orchard *et al*., 2007a, fig. 19; Carter and Orchard, 2007, pl. 2, figs. 12, 13, 16–18.

Material examined.—One specimen, KMSP-100019, from QU3-163.

Remarks.—This morphotype is characterized by relatively long element and has some accessory nodes on the posterior platform. In contrast to morphotype A, morphotype B has a broader and more ornate platform. Morphotype C has more carinal nodes posterior of a pair lateral nodes.

Mockina postera (Kozur and Mostler, 1971)

Figure 8.11

Gladigondolella abneptis (Huckriede), Hayashi, 1968, pl. 2, fig. 6 (only).

Tardogondolella abneptis postera Kozur and Mostler, 1971, p. 14, 15, pl. 2, figs. 4–6.

Metapolygnathus posterus posterus (Kozur and Mostler), Kozur, 1972, pl. 6, figs. 23 (only).

Epigondolella postera (Kozur and Mostler), Krystyn, 1973, p. 141, pl. 5, figs. 5, 6; Budurov, 1977, p. 43, 44, pl. 5, figs. 25, 26; Isozaki and Matsuda, 1980, figs. 6, 7; Cafiero and Bonardi, 1981, pl. 58, figs. 21, 22; Ishida, 1981, pl. 7, figs. 1, 2; Isozaki and Matsuda, 1982, p. 115–117, pl. 3, figs. 1–7; Orchard, 1983, p. 186, fig. 15.P–R; Orchard in Carter *et al*., 1989, pl. 1, fig. 15; Budurov and Sudar, 1990, pl. 5, figs. 1–5; Orchard, 1991a, pl. 4,

fig. 21; Orchard, 1991b, p. 310, pl. 4, figs. 16–19; Nicoll and Foster, 1994, p. 108, figs. 7.3-7.5; Krystyn *et al.*, 2009, fig. 4.5.

Epigondolella postera hayashii Kozur and Mostler, Sweet in Ziegler, 1977, p. 191.

Metapolygnathus posterus (Kozur and Mostler), Gupta *et al.*, 1980, p. 593, pl. 2, figs. 7, 8, pl. 5, figs. 1–9; Gaździcki *et al.*, 1979, pl. 5, fig. 14; Kovács and Kozur, 1980, pl. 14, fig. 7.

Mockina postera (Kozur and Mostler), Ishida and Hirsch, 2001, p. 238, pl. 4, figs. 4, 6 (non fig. 2); Moix *et al*., 2007, pl. 1, fig. 3; Ishida *et al.*, 2015, p. 13, pl. 2, fig. 5, pl. 3, figs. 1, 2, (non fig. 4).

Epigondolella sp. cf. *postera* Kozur, Katvala and Stanley, 2008, p. 222, fig. 42.9.

Material examined.—One specimen, KMSP-100020, from NHR-40.

Description.—The P_1 element is relatively small, and characterized by an asymmetrical posterior platform margin. The platform is about half of the entire element. The anterior platform bears one or two sharp denticles on each margin. In profile, the blade is composed of about 5 denticles, and rises from both anterior and posterior ends. Relatively low carinal nodes may be continuous to the posterior platform margin, and form a pointed posterior end of the platform. The pit lies in the anterior half of the platform within the keel, which has a pointed termination.

Remarks.—The described specimen has one denticle on one anterior platform margin and two denticles on the other. Asymmetrical posterior platform margin has no ornamentation

except for the carnal nodes. These features match well with the holotype (Kozur and Mostler, 1971, pl. 2, fig. 4)

Mockina slovakensis (Kozur, 1972)

Figure 8.12

Metapolygnathus slovakensis Kozur, 1972, p. 10, pl. 7, fig. 23.

Epigondolella multidentata Mosher, Budurov and Sudar, 1990, pl. 5, figs. 20–22 (only).

Mockina slovakensis (Kozur), Channell *et al*., 2003, pl. A2, figs. 56, 57, 58 (only); Mazza *et al*., 2012b, p. 121, pl. 7, figs. 9, 10; Rigo *et al.*, 2016, fig. 3.2.

Material examined.—One specimen, KMSP-100021, from NHR-112.

Description.—One broken P_1 element has an oval platform with thick platform margins, which bear some high denticles. The blade forms a high crest and abruptly descends onto the platform as a row of carinal nodes. The pit lies below the center of the platform, and anterior to the rounded posterior end of the keel.

Remarks.—The described specimen is characterized by an abrupt step between the blade and the carina, and an oval platform with thick platform margins. These distinctive features enable it to be assigned to the species.

Mockina spiculata **(**Orchard, 1991b)

Figures 8.13, 8.14

Epigondolella C population Orchard, 1983, p. 185, fig. 15M–O; Orchard, 1991a, pl. 4, figs. 18–20.

Epigondolella spiculata Orchard, 1991b, p. 312, pl. 3, figs. 10, 14, 15; Nicoll and Foster, 1994, p. 108, 109, fig. 8.4; Channell *et al*., 2003, pl. A2, figs. 38, 42; Katvala and Stanley, 2008, p. 223, fig. 42.1–42. 7.

Material examined.—Two specimens, KMSP-100022, 100023, from NCU-541.

Description.—The P_1 elements are characterized by an ornate, subrectangular and asymmetrical platform with a length-to-breadth ratio of 2:1, a slightly sinuous longitudinal axis. The blade descends onto the platform and abruptly terminates on the anterior platform. The carinal nodes become larger towards the posterior end, and reach to the posterior end of the platform. The serrated posterior platform margin has several additional nodes. Each anterior lateral platform bears 3–4 well developed, discrete, and sharp denticles. The pit lies anterior of the platform midlength within relatively broad basal keel.

Remarks.—Orchard (1983) distinguished *Epigondolella* C population from Middle Norian specimens that previously assigned to *E. abneptis*. *E. spiculata* was differentiated from *Epigondolella* C population by Orchard (1991b) based on the characteristic platform shape and ornamentation. The described specimens may be primitive form of this species because of less ornamentation on the posterior platform margin. This species has the typical characters of the

genus *Mockina*, being characterized by a reduced, elliptic platform with sharp denticles, anteriorly sifted pit and a pointed or narrowly rounded posterior platform margin and keel termination.

Mockina aff. ***zapfei*** (Kozur, 1973)

Figure 9.1

aff. *Metapolygnathus* n sp. Kozur, 1972, pl. 7, fig. 1.

Metapolygnathus aff. *posterus* (Kozur and Mostler), Kozur, 1972, pl. 7, fig. 2.

Metapolygnathus zapfei Kozur, 1973, p. 18–20; Gaździcki *et al*., 1979, pl. 5, fig. 15.

Epigondolella postera Kozur and Mostler, Budurov and Sudar, 1990, pl. 5, figs. 6–8 (only).

Epigondolella slovakensis Kozur and Mock, Martini *et al.*, 2000, pl. V, figs. 13, 14 (only).

Mockina zapfei (Kozur), Channell *et al*., 2003, pl. A2, fig. 55 (only); Rigo *et al*., 2016, fig. 3.1.

Material examined.—One specimen, KMSP-100024, from QU3-163.

Description.—The P_1 element has a rectangular platform with a length-to-breadth ratio of 2:1. The platform is about one half of the total unit length, and characterized by an asymmetrical posterior platform margin whose one side is pointed. The row of 6–7 carinal nodes is curved on the posterior platform and extends to the pointed posterior end of the

platform. The lateral margins bear 2–3 sharp denticles on each side. In profile, the blade is composed of 7-8 denticles and forms a high convex crest. The pit lies anterior of the platform midlength. The keel end is bifurcated.

Remarks.—The described specimen is very similar to *Mockina zapfei*, but we regarded it as affinis of this species because it has a broader platform with more denticles on the lateral platform margin. The tapered posterior platform margin, shape denticles and anteriorly sifted pit of this specimen are similar to that of type species of the genus *Mockina*. *E. spiculata* also resembles this specimen, but the blade which is highest at the anterior end and abruptly ends. The pit of the *Primatella asymmetrica* is subcentral and lies within the keel that has a pointed termination.

Mockina sp. indet. A

Figures 9.2, 9.3

Material examined.—Two specimens, KMSP-100025, from NHR-130 and KMSP-100026, from NHR-55.

Description.—The P_1 elements have a long subrectangular platform with a length-to-breadth ratio of between 2:1 and 2.5:1, two distinct denticles on one anterior platform margin and one on the other. A constriction may occur in the center of the platform. The posterior platform is commonly inornate. The pit is situated beneath the anterior part of the

platform and far anterior of the relatively broad keel. The basal keel is slightly carved around the pit.

Remarks.—The features of this species indicate a close phylogenetic relationship with *Mockina postera*. The first appearance of *M.* sp. indet. A occurs higher than that of *M. postera* in the section N. This evidence suggests that *M.* sp. indet. A probably evolved from *M. postera* during Late Norian time. This species resembles *M. postera*, but differ in having a longer posterior platform. *M. elongata* and *Epigondolella matthewi* are also similar to this species, but *M. elongata* has a more slender platform, and *E. matthewi* has more denticles on each anterior platform and a biconvex platform.

Mockina sp. indet. B

Figures 9.4–9.6

Material examined.—Three specimens, KMSP-100027, from QU3-163, KMSP-100028, from NHR-42, KMSP-100029, from NHR-57.

Description.—The P_1 elements are characterized by an elongate platform shaped like a rhombus, broadest in the medial part, and with a length-to-breadth ratio close to 2:1. The ornamentation is restricted to the anterior part of the platform margin and consists of 3–4 pointed denticles, the posteriormost of which is the largest. The blade is approximately 1/3 total element length with 5–6 partly fused denticles forming a high crest, and descends onto the platform as a row of about five nodes that extend to the pointed posterior platform margin.

Remarks.—The slender platform of *Mockina* sp. indet. B is similar to those of *M. mosheri* and juveniles of *E. multidentata*, but the platform of *M. mosheri* has a curved longitudinal axis and less denticles on the anterior platform margin, and the platform of *E. multidentata* is broadest in the anterior. The present species also resembles *M. bidentata*, but differ in having a broader platform and more denticles on the anterior platform margin.

Genus ***Neogondolella*** Bender and Stoppel, 1965

Type species.—*Gondolella mombergensis* Tatge, 1956.

Neogondolella cf. ***liardensis*** Orchard, 2007a

Figure 9.7

cf. *Neogondolella inclinata* (Kovács), Orchard, 2005, p. 85, text-fig. 11; Orchard, 2006, pl. 6, figs. 1, 2, 9, 10.

Neogondolella liardensis Orchard, 2007a, p. 328, figs. 3.4–3.6.

Material examined.—One specimen, KMSP-100030, from NCL-185.

Description.—One broken P_1 element typically has a narrow, long platform with a length-to-breadth ratio of about 6:1, no ornamentation except for microreticulation, and subparallel margins that gradually reduced to the anterior end of the blade. The blade is

composed of partly fused denticles that are higher to the anterior, and passes posteriorly into low, highly fused carinal nodes. In lateral view, the element is arched and a prominent cusp lies in front of the posterior platform margin. The pit underlies the posterior part of the platform.

Remarks.—The described specimen has a higher blade and more fused carinal nodes than *N. liardensis*. This variation may be intraspecific because large populations of this species show variation in carinal development according to Orchard (2007a).

Genus ***Paragondolella*** Mosher, 1968a

Type species.—*Paragondolella excelsa* Mosher, 1968a.

Paragondolella auriformis (Kovács, 1977)

Figure 9.8

Gondolella auriformis Kovács, 1977, p. 78, pl. 1, figs. 4, 5, pl. 2, fig. 1, pl. 3, fig. 1, pl. 8, fig. 1; Kovács and Kozur, 1980, pl. 8, figs. 5, 6, pl. 9, fig. 1; Krystyn, 1983, p. 242, pl. 5, figs. 5, 6, pl. 6, fig. 1 (only); Kovács, 1986, p. 214, pl. 11, figs. 1, 2 (only); Kovács *et al.*, 1989, p. 48, fig. 4a.

Neogondolella auriformis (Kovács), Chhabra and Kumar, 1992, pl. 4, fig. 12.

Metapolygnathus auriformis (Kovács), Mastandrea , 1995, p. 499, pl. 1, figs. 6–9; Hauser *et al.*, 2001, pl. 1, fig. 12; Hornung *et al*., 2007, p. 280, fig. 7g, h.

Paragondolella auriformis (Kovács), Rigo *et al*., 2007, fig. 4.9.

Material examined.—One specimen, KMSP-100031, from NCU24.

Description.—The P_1 element is characterized by a relatively short, ear-like platform with no ornamentation except for microreticulation, and a distinct posterior platform constriction. The blade is about 1/2 of the total element length, composed of 7 denticles and forms a high convex crest. The anterior trough margin is weakly-developed and the free blade is long. The terminal carinal node is surrounded by a narrow platform rim. The pit lies in the posterior half of the platform within the keel, that is posteriorly rounded.

Remarks.—This specimen is assigned to *Paragondolella*, because it has an inornate platform, a rounded posterior margin and a posteriorly located pit. *P. auriformis* is similar to *P.? tadpole*, but differ in having a distinct platform constriction.

Paragondolella inclinata (Kovács, 1983)

Figures 10.1, 10.2

Gondolella foliata inclinata Kovács, 1983, p. 110–112, pl. 1, figs. 1–4; pl. 3, fig. 2.

Paragondolella inclinata (Kovács), Orchard, 2007a, p. 328, figs. 3.1–3.3.

Material examined.—Two specimens, KMSP-100033, from NCL-2 and KMSP-100034, from NCL-128.

Description.—The broken P_1 elements are characterized by a long platform and a high blade-carina. The platform margin is covered by microreticulation and has no marginal nodes. The platform tapers gradually to the anterior without geniculation. The high blade-carina is composed highly fused denticles and forms an arcuate crest. The pit lies in the posterior half of the platform within the keel, which has a subrectangular termination.

Remarks.—The high blade-carina and a tapered platform without geniculation are diagnostic features, which enable us to distinguish this species. *Paragondolella inclinata* is similar to *P. praelindae*, but differ in having no distinct platform constriction.

Paragondolella*? *tadpole (Hayashi, 1968)

Figure 9.9

Gondolella tadpole Hayashi, 1968, p. 71, pl. 1, fig. 6; Kozur, 1972, pl. 3, figs. 7, 8, pl. 6, fig. 1; Kozur, 1974, p. 12, Kovács and Kozur, 1980, pl. 9, figs. 4, 5; Hornung, 2006, fig. 7.2; Hornung and Brandner, 2005, fig. 9f.

Neogondolella cf. *tadpole* (Hayashi), Koike, 1981, pl. 2, figs. 18, 19.

Metapolygnathus tadpole (Hayashi), Orchard, 2006, pl. 4, figs. 1–3, pl. 6, 11, 12, 15, 16; Orchard, 2007a, p. 326, figs. 3.19–3.21; Orchard and Balini, 2007, figs. 6.12, 6.13, 6.20, 6.21.

Paragondolella tadpole (Hayashi), Rigo *et al.*, 2007, fig. 4.8; Muttoni *et al.*, 2014, figs. 3.A, 3.D.

Material examined.—One specimen, KMSP-100032, from NCU-18.

Description.—The P_1 element is characterized by a relatively small, subrectangular to oval, inornate platform with a length-to-breadth ratio of between 1.5:1 and 2:1. The blade is about 1/2 of the total element length, composed of about 6 denticles that are highest near anterior third, and descend onto the platform as a row of discrete, prominent nodes, which terminate in front of the posterior end of the element. In profile, the element is arched, and the carinal nodes project above the level of the slightly raised lateral platform margin. The pit lies in a posterior position with respect to both the platform and keel, which has a rounded to subrectangular termination.

Remarks.—The described specimen resembles the holotype of *tadpole* reported by Hayashi (1968) but the described specimen has a distinct geniculation points and the long blade is broken. This species is regarded as a transitional form between the genera *Paragondolella* and *Quadralella* by Chen *et al*. (2015) because it has intermediate characters to typical *Quadralella* species. We follow Chen *et al*. (2015) in treating *Paragondolella*? *tadpole* (Hayashi).

Paragondolella aff. ***praelindae*** Kozur, 2003

Figure 10.3

aff. *Paragondolella praelindae* Kozur, 2003, p. 71, pl. 1, fig. 4; Channell *et al*., 2003, pl. A1, fig. 3; Rigo *et al.*, 2007, figs. 4.10, 4.11; Mazza *et al.*, 2012b, p. 126, pl. 7, fig. 13; Muttoni *et al.*, 2014, fig. 3E.

Material examined.—One specimen, KMSP-100035, from NCL-2.

Description.—The P_1 element is characterized by a broad, inornate platform with a marked constriction in the posterior 1/7 of the platform, biconvex lateral platform margin, no geniculation point, and a length-to-breadth ratio of about 3:1. The free blade is generally absent due to the development of anterior tapered platform. Laterally the profile of the element is arched. The blade is composed of fused denticles, forms a convex crest, and passes posteriorly into low carinal nodes. The pit is situated near the constriction portion of the platform and subterminal within the keel that is posteriorly rounded.

Remarks.—*Paragondolella lindae* is similar to this species, but differ in having a more abrupt anterior narrowing of the platform and a more slender platform.

Genus ***Parvigondolella*** Kozur and Mock, 1972

Type species.—*Parvigondolella andrusovi* Kozur and Mock, 1972.

Parvigondolella andrusovi Kozur and Mock, 1972

Figure 10.4

Parvigondolella andrusovi Kozur and Mock, 1972, p. 5, pl. 1, figs. 11, 12; Kozur and Mostler, 1972, pl. 4, fig. 6; Kozur, 1972, pl. 7, fig. 10; Gaździcki *et al.*, 1979, pl. 5, figs. 8, 9; Kovács and Kozur, 1980, pl. 15, fig. 3; Krystyn, 1980, pl. 14, figs. 4–6; Isozaki and Matsuda, 1982, pl. 4, figs. 6, 7; Nagao and Matsuda, 1982, pl. 1, figs. 5, 6; Isozaki and Matsuda, 1983, p. 69–71, pl. 4, figs. 1–7 (only); Channell *et al*., 2003, pl. A2, figs. 50, 52, 59, 60, pl. A3, figs. 1, 2, 73, 80, 81, 82; Bertinelli *et al*., 2005, fig. 4.6; Rigo *et al*., 2005, figs. 5.5, 5.6; Balini *et al*., 2010, pl. 4, fig. 10; Gale *et al*., 2012, fig. 4.O; Mazza *et al*., 2012b, pl. 7, fig. 14.

Epigondolella bidentata, Krystyn, 1980, pl. 14, figs. 5, 6 (only); Budurov and Sudar, 1990, pl. 5, fig. 12 (only).

Material examined.—One specimen, KMSP-100036, from NHR-53.

Description.—The small P_1 element has no platform and a blade composed of 8 partially fused denticles, which tends to be highest in the anterior one-third of the blade. The cusp is larger than the other denticles and never situated on the posterior end of the element. In profile, the element is slightly arched in the posterior one-third. The pit lies posterior of the element midlength.

Remarks.—Although the described specimen is partially broken, it has 8 denticles and the cusp, which is situated never terminal in position and larger than other denticles. These features match well with holotype of Kozur and Mock (1972, pl. 1, fig. 11).

Parvigondolella aff. ***vrielyncki*** Kozur and Mock, 1991

Figure 10.5

aff. *Epigondolella bidentata*, Krystyn, 1980, pl. 14, fig. 4 (only).

Parvigondolella andrusovi, Vrielynck, 1981, p. 217, pl. 7, figs. 19, 20.

Parvigondolella? *vrielyncki* Kozur and Mock, 1991, p. 276.

Parvigondolella vrielyncki Kozur and Mock, Channell *et al*., 2003, pl. A2, fig. 49.

Material examined.—One specimen, KMSP-100037, from NHR-53

Description.—The blade is composed of 11–12 denticles that are often highest in the anterior part and its height gradually decreases toward the posterior end. In lateral view, this element is straight or slightly arched. The pit lies posterior of the element midlength.

Remarks.—Kozur and Mock (1991) established the *Parvigondolella vrielyncki* and chose the juvenile specimen of *Epigondolella bidentata* illustrated by Krystyn (1980, pl. 14, fig. 4) as holotype of this species. The described specimen is regarded as affinis because it is very similar to *P. vrielyncki*, but differ in having the cusp, which is penultimate denticle and larger than the other denticles. This specimen also resembles *Parvigondolella andrusovi*, but it has a longer blade, which is composed of more denticles than the latter.

Genus ***Primatella*** Orchard 2013

Type species.—*Epigondolella primitia* Mosher, 1970.

Primatella orchardi (Kozur, 2003)

Figures 10.6, 10.7

Epigondolella orchardi Kozur, 2003, p. 69, pl. 1, figs. 1, 7 (only).

Primatella orchardi (Kozur), Carter and Orchard, 2013, figs. 7.4–7.6; Balini *et al*., 2014, fig. 10.h; Orchard, 2014, figs. 70.1–70.26.

Material examined.—Two specimens, KMSP-100038, from N-130 and KMSP-100039, from NCU-186.

Description.—The P_1 elements have a subrectangular platform with a length-to-breadth ratio of between 1.5:1 and 2:1, and an indentation of the lateral margins in the posterior 1/3 to 1/2 of the platform. The anterior platform margin bears 2–3 round to laterally enlarged, pointed and discrete nodes. The breadth of the posterior and anterior platform may be greater than that of the anterior platform. The pit is medial to posterior in position, and anterior of the posterior end of the keel, which is commonly bifurcated.

Remarks.—These elements differ from *Q. postlobata* in their pointed marginal nodes, relatively shorter platform, and bifurcated posterior end of the keel.

Genus ***Quadralella*** Orchard 2013

Type species.—*Quadralella lobata* Orchard, 2014.

Quadralella carpathica (Mock, 1979)

Figures 10.8, 10.9

Gondolella carpathica Mock, 1979, p. 172, pl. 1, figs. 1–5.

Paragondolella carpathica (Mock), Martini *et al.*, 1991, pl. 19 figs. 1-9; Channell *et al*., 2003, pl. A1, figs. 4, 5, 9, 10 (only).

Metapolygnathus carpathicus (Mock), Orchard, 2006, pl. 7, figs. 1, 2; Orchard, 2007b, figs. 1.10–1.12; Orchard, 2007c, pl. 1, figs. 24, 25, 29–31 (only).

Metapolygnathus ex gr. *polygnathiformis* (Budurov and Stefanov), Orchard, 2006, pl. 4, figs. 1–3.

Metapolygnathus polygnathiformis (Budurov and Stefanov), Orchard, 2007b, figs. 1.19–1.21.

Carnepigondolella angulata Mazza *et al*., 2012a, p. 416, fig. 9B (only).

Carnepigondolella carpathica (Mock), Balini *et al*., 2010, pl. 2, fig. 5; Mazza *et al*., 2012b, p. 93, pl. 1, figs. 2, 3.

Quadralella carpathica (Mock)**,** Orchard, 2014, p. 108, figs. 76.1–76.15.

Material examined.—Two specimens, KMSP-100040, from QU2-62 and KMSP-100041, from N-115.

Description.—P_1 elements have a relatively large, broad subrectangular platform with a length-to-breadth ratio of 2:1, poorly differentiated nodes on each anterior platform margin, and subparallel lateral margin. The platform is 2/3–3/4 total element length. The tapered platform flange extend close to the anterior end of the blade, which is highly fused, highest near the anterior end, and descends onto the platform as a row of discrete carinal nodes. Laterally, the element is arched with a downturned posterior platform, which is inornate except for microreticulation. The pit lies in the posterior half of the platform and shifted anteriorly with respect to the keel end, which is subtriangular or bifurcated.

Remarks.—These distinctive features match well the morphotype of Mock (1979, figs. 1–5), except for the shape of the keel end. *Quadralella tuvalica* has raised anterior platform margins with more developed nodes, which may reach the center of the platform.

Quadralella noah (Hayashi, 1968)

Figures 11.1, 11.2

Metapolygnathus noah Hayashi, 1968, p. 72, pl. 3, fig. 10; Orchard, 2007b, figs. 1.25–1.27.

Paragondolella noah (Hayashi), Noyan and Kozur, 2007, fig. 5.5 (only).

Paragondolella polygnathiformis noah (Hayashi), Rigo *et al*., 2007, fig. 4.6.

Quadralella noah (Hayashi), Orchard, 2014, p. 114, figs. 81.1–81.18.

Material examined.—Two specimens, KMSP-100042, from NCU-70 and KMSP-100043, from QU1-88.

Description.—Two broken P_1 elements have a long and subrectangular platform with a length-to-breadth ratio of between 2.5:1 and 3:1. The blade is 1/3 of total element length and the anterior trough margin extends nearly to the anterior end of the blade. The platform margins are covered by microreticulae, and lateral margins are parallel to subparallel. The anterior platform margin is slightly raised and has a few weakly-developed nodes. The pit is the posterior part of the platform and anteriorly situated within the keel that has a subrectangular or weakly bifurcated termination.

Remarks.—The described specimens are similar to *Quadralella tuvalica*, but differ having a few weakly-developed nodes that are confined to the anteriormost 1/4 of the platform.

Quadralella postlobata Orchard, 2014

Figures 11.5, 11.6

Neogondolella polygnathiformis (Budurov and Stefanov), Koike, 1982, p. 25, pl. 1, figs. 2, 3, 7 (only).

Metapolygnathus nodosus (Hayashi), Orchard, 2007c, pl. 1, figs. 11–16 (only); Katvala and Stanley, 2008, fig. 39.28.

Metapolygnathus carpathicus (Mock), Katvala and Stanley, 2008, fig. 39.12.

Quadralella postlobata Orchard, 2014, p. 118, figs. 80.14–80.40.

Material examined.—Two specimens, KMSP-100046, from NCU-130 and KMSP-100047, from N-121.

Description.—Two broken P_1 elements are characterized by rectangular platform with a length-to-breadth ratio of between 2:1 and 2.5:1, and a distinct constriction in the posterior 1/3 of the platform. The raised anterior platform margins have 3–4 poorly developed and rounded nodes. The posteriormost carina surrounded by the posterior platform margin. The pit underlies the posterior half of the platform and close to the posterior end of the keel that is rectangular or weakly bifurcated.

Remarks.—This species is closely similar to *Quadralella lobata*, which is its proposed precursor, but differ in having more raised lateral platform margins, shorter platform, longer blade and a more anteriorly located constriction.

Quadralella tuvalica (Mazza and Rigo, 2012)

Figures 11.3, 11.4

Neogondolella polygnathiformis (Budurov and Stefanov) Koike, 1982, p. 25, pl. 1, figs. 10, 11 (only).

Metapolygnathus nodosus (Hayashi) Orchard, *in* Carter *et al.,* 1989, pl. 1, fig. 3; Carter and Orchard, 2000, pl. 1, fig. 1; Orchard, 2007b, figs. 1.1–1.3; Orchard , 2007c, pl. 1, figs. 14–19 (only).

Carnepigondolella tuvalica Mazza and Rigo *in* Mazza *et al*., 2012b, p. 100, pl. 3, figs. 3–5, 9, 10 (only).

Quadralella tuvalica (Mazza and Rigo) Carter and Orchard, 2013, figs. 3.20–3.22; Orchard, 2014, figs. 88.1–88.24.

Material examined.—Two specimens, KMSP-100044, from QU2-63 and KMSP-100045, from N-130.

Description.—The P_1 elements have a subrectangular platform with a length-to-breadth ratio of 2:1 and subparallel lateral margin. The anterior platform margin bears 3-4 low, rounded nodes, which reach the middle of the platform. The anterior trough margin extends close to the anterior end of the blade. The blade is about 1/3 total element length and passes onto the platform as 5–7 carinal nodes. In lateral view, the elements are arched with a downturned posterior platform. The pit lies close to the posterior end of the keel or anteriorly shifted within the keel, which is squared or bifurcated.

Remarks.—This species was differentiated by Mazza and Rigo (in Mazza *et al*, 2012b) from a variety of form that had been referred to *Quadralella nodosus* (*Carnepigondolella* in Mazza *et al*, 2012b). Although the holotype of *Q. tuvalica* illustrated by Mazza *et al.* (2012b) has a slightly rounded posterior platform margin, Orchard (2014) restricted *Q. tuvalica* to forms

with a more rectangular posterior platform margin, and assigned the holotype of Mazza *et al.* (2012b) to *Primatella rotunda* as new species. The described specimens resemble *Primatella rotunda*, but we assigned to *Q. tuvalica* based on the description of Mazza *et al.* (2012b). The morphological features of *Q. tuvalica* are an elevated anterior platform margin and relatively broad anterior trough margin that extend close to the anterior end of the blade. Although the described specimens have less elevated anterior platform margin, they share many features with *Q. tuvalica*. The described specimens are similar to *Q. nodosus*, but differ in having a longer blade. Compared with *Carnepigondolella milanae*, this species has a shorter free blade and an upturned platform margin.

Quadralella sp. indet A

Figures 11.7

Material examined.—One specimen, KMSP-100048, from NCU-131.

Description.—The P_1 element has a relatively broad, sub-rectangular platform without ornamentation, except for microreticulation. The anterior trough margin is broad and extends the anterior end of the blade. Overall platform shape is subparallel, with the broadest point lying a platform midlength. There are a tiny step and a geniculation point at anterior platform margin. The blade is composed of about 7 denticles and forms a convex crest. The cusp is the terminal and highest carinal nodes. The pit is situated posterior position with respect to both the platform and keel end, which is subrectangular.

Remarks.—The features of this species indicate a close phylogenetic relationship with *Quadralella polygnathiformis,* but this species differ in overall platform shape and having no irregular step at anterior platform margin.

Acknowledgements

We thank Satoshi Yamakita and Satoshi Takahashi for assistance in the identification of conodonts. Manuel Rigo kindly reviewed an earlier draft of our manuscript. Michael J. Orchard and an anonymous reviewer provided constructive comments and suggestions which improved the manuscript. Financial support by the grant-in-aid for scientific research by the Japan Society for the Promotion of Science (# 15H05771, 26707027) to T. Onoue is greatly acknowledged.

References

Amodeo, F., 1999: Il Triassico terminale - Giurassico del Bacino Lagonegrese. Studi stratigrafici sugli Scisti Silicei della Basilicata (Italia meridionale). *Mémoires de Géologie (Lausanne)*, vol. 33, p. 1–121.

Ando, A., Kodama, K. and Kojima, S., 2001: Low-latitude and Southern Hemisphere origin of Anisian (Triassic) bedded chert in the Inuyama area, Mino terrane, central Japan. *Journal of Geophysical Research*, vol. 106, p. 1973–1986.

Balini, M., Bertinelli, A., Di Stefano, P., Guaiumi, C., Levera, M., Mazza, M., Muttoni, G., Nicora, A., Preto, N. and Rigo, M., 2010: The Late Carnian–Rhaetian succession at Pizzo

Mondello (Sicani Mountains). *Albertiana*, vol. 39, p. 36–58.

Balini, M., Jenks, J. F., Martin, R., McRoberts, C. A., Orchard, M. J. and Silberling, N. J., 2014: The Carnian/Norian boundary succession at Berlin-Ichthyosaur State Park (Upper Triassic, central Nevada, USA). *Pal.o ntologische Zeitschrift*, vol. 89, p. 399–433.

Bender, H. and Stoppel, D., 1965: Perm-Conodonten. *Geologisches Jahrbuch*, vol. 82, p. 331–364.

Bertinelli, A., Ciarapica, G., De Zanche, V., Marcucci, M., Mietto, P., Passeri, L., Rigo, M. and Roghi, G., 2005: Stratigraphic evolution of the Triassic-Jurassic Sasso di Castalda succassion (Lagonegro Basin, Southern Apennines, Italy). *Bollettino della Societa Geologica Italiana*, vol. 124, p. 161–175.

Budurov, K. J., 1972: *Ancyrogondolella triangularis* gen et sp. n. (Conodonta). *Mitteilungen der Gesellschaft der Geologie und Bergbaustudenten*, vol. 21, p. 853–860.

Budurov, K. J., 1976: Structures, evolution and taxonomy of the Triassic platform conodonts. *Geologica Balcanica*, vol. 6, p. 13–20.

Budurov, K. J., 1977: Revision of the late Triassic platform conodonts. *Geologica Balcanica*, vol. 7, p. 31–48.

Budurov, K. J. and Sudar, M. N., 1990: Late Triassic Conodont Stratigraphy. *Courier Forschungsinstitut Senckenberg*, vol. 118, p. 203–239.

Buryi, G. I., 1996: Evolution of Late Triassic conodont platform elements. *Acta Micropalaeontologica Sinica*, vol. 13, p. 135–142.

Buryi, G. I., 1997: Triassic conodont biostratigraphy of the Sitkhote-Alin. *Memoires de*

Geologie (Lausanne), no. 30, p. 45–60.

Cafiero, B. and De Capoa Bonardi, P., 1981: I conodonti dei calcari ad Halobia del Trias superiore del Montenegro (Crna-Gora, Jugoslavia). *Rivista Italiana di Paleontologia e Stratigrafia*, vol. 86, p. 563–576.

Carter, E. S. and Orchard, M. J., 2000: Intercalibrated conodont-radiolarian biostratigraphy and potential datums for the Carnian/Norian boundary within the Upper Triassic Peril Formation, Queen Charlotte Islands. *Geological Survey of Canada Current Research*, no. 2000-A07, p. 1–11.

Carter, E. S. and Orchard, M. J., 2007: Radiolarian–conodont–ammonoid intercalibration around the Norian–Rhaetian Boundary and implications for trans-Panthalassan correlation. *Albertiana*, vol. 36, p. 146–159.

Carter, E. S. and Orchard, M. J., 2013: Intercalibration of conodont and radiolarian faunas from the Carnian-Norian boundary interval in Haida Gwaii, British Columbia, Canada. *New Mexico Museum of Natural History and Science Bulletin*, no. 61, p. 67–92.

Carter, E. S., Orchard, M. J. and Tozer, E. T., 1989: Integrated ammonoid-conodont-radiolarian biostratigraphy, Late Triassic Kunga Group, Queen Charlotte Islands, British Columbia. *Geological Survey of Canada Paper*, no. 89-1H, p. 23–30.

Channell, J. E. T., Kozur, H. W., Sievers, T., Mock, R., Aubrecht, R. and Sykora, M., 2003: Carnian-Norian biomagnetostratigraphy at Silická Brezová (Slovakia): Correlation to other Tethyan sections and to the Newark Basin. *Palaeogeography*, *Palaeoclimatology*, *Palaeoecology*, vol. 191, p. 65–109.

Chen, Y., Krystyn, L., Orchard, M., Lai, X. and Richoz, S., 2015: A review of the evolution, biostratigraphy, provincialism and diversity of Middle and early Late Triassic conodonts. *Papers in Palaeontology*, vol. 2, p. 235–263.

Chhabra, N. L. and Kumar, S., 1992: Late Scythian through Early Carnian conodont assemblages and their biostratigraphic importance from off shore carbonates of northern Kumaun, Tethys Himalaya, India. *Revue de Micropaléontology*, vol. 35, p. 3–21.

Dzik, J., 1976: Remarks on the evolution of Ordovician conodonts. *Acta Palaeontologica Polonica*, vol. 21, p. 395–455.

Eichenberg, W., 1930: Conodonten aus dem Culm des Harzes. *Paläontologische Zeitschrift*, vol. 12, p. 177–182.

Epstein, A. G., Epstein, J. B. and Harris, L. D., 1977: Conodont color alteration: an index to organic metamorphism. *United States Geological Survey professional paper*, no. 995, p. 1–27.

Gale, L., Kolar-Jurkovšek, T., Šmuc, A. and Rožič, B., 2012: Integrated Rhaetian foraminiferal and conodont biostratigraphy from the Slovenian Basin, eastern Southern Alps. *Swiss Journal of Geosciences*, vol. 105, p. 435–462.

Gaździcki, A., Kozur, H. and Mock, R., 1979: The Norian-Rhaetian boundary in the light of micropaleontological data. *Geologija*, vol. 22, p. 71–112.

Giordano, N., Rigo, M., Ciarapica, G. and Bertinelli, A., 2010: New biostratigraphical constraints for the Norian/Rhaetian boundary: data from Lagonegro Basin, Southern Apennines, Italy. *Lethaia*, vol. 43, p. 573–586.

Gupta, V. J., Kovács, S., and Scheffer, A. O., 1980: Upper Triassic microfossils from northeastern Kumaun Himalaya, India. *Recent Researches in Geology*, vol. 6, p. 582–593.

Hauser, M., Martini, R., Burns, S., Dumitraca, P., Krystyn, L., Matter, A., Peters, T. and Zaninetti, L., 2001: Triassic stratigraphic evolution of the Arabian-Greater India embayment of the southern Tethys margin. *Eclogae Geologicae Helvetiae*, vol. 94, p. 29–62.

Hayashi, S., 1968: The Permian conodonts in chert of the Adoyama Formation, Ashio Mountains, central Japan. *Earth Science (Chikyu Kagaku)*, vol. 22, p. 63–77. (*in Japanese with English abstract*)

Hornung, T., 2006: Die Reingrabener Wende in der Halleiner Salzbergfazies (distale Hallstattfazies)–biostratigraphische Daten. *Geo.Alp*, vol. 3, p. 9–21.

Hornung, T., and Brandner, R., 2005: Biochronostratigraphy of the Reingraben Turnover (Hallstatt Facies Belt): Local black shale events controlled by regional tectonics, climatic change and plate tectonics. *Facies*, vol. 51, p. 460–479.

Hornung, T., Spatzenegger, A. and Joachimski, M. M., 2007: Multistratigraphy of condensed ammonoid beds of the Rappoltstein (Berchtesgaden, southern Germany): unravelling palaeoenvironmental conditions on 'Hallstatt deep swells' during the Reingraben Event (Late Lower Carnian). *Facies*, vol. 53, p. 267–292.

Huckriede, R., 1958: Die Conodonten der Mediterranen Trias und ihr stratigraphischer Wert. *Paläontologische Zeitschrift*, vol. 32, p. 141–175.

Igo, H. and Nishimura, H., 1984: The Late Triassic and Early Jurassic radiolarian

biostratigraphy in the Karasawa, Kuzuu town, Tochigi Prefecture (Preliminary report). *Bulletin of Tokyo Gakugei University*. *Section IV*, vol. 36, p. 173–193. (*in Japanese with English abstract*)

Ikeda, M. and Tada, R., 2014: A 70 million year astronomical time scale for the deep-sea bedded chert sequence (Inuyama, Japan): Implications for Triassic–Jurassic geochronology. *Earth and Planetary Science Letters*, vol. 399, p. 30–43.

Ishida, K., 1979: Studies of the South Zone of the Chichibu Belt in Shikoku, Part II -Stratigraphy and Structure Around Nagayasu-guchi Dam, Tokushima Prefecture-. *Journal of Science, University of Tokushima*, vol. 12, p. 61–92. (*in Japanese with English abstract*)

Ishida, K., 1981: Fine stratigraphy and conodont biostratigraphy of a bedded-chert member of the Nakagawa Group. *Journal of Science, University of Tokushima*, vol. 14, p. 107–137. (*in Japanese with English abstract*)

Ishida, K. and Hirsch, F., 2001: Taxonomy and faunal affinity of Late Carnian-Rhaetian conodonts in the Southern Chichibu Belt, Shikoku, SW Japan. *Rivista Italiana di Paleontologia e Stratigrafia,* vol. 107, p. 227–250.

Ishida, K., Suzuki, S., Dimalanta, C. B., Yumul Jr, G. P., Zamoras, L. R., Faure, M., Hirsch, F., Kiliç, A. M. and Placencia, P., 2015: Discovery of Triassic microfossils from the Buruanga Peninsula, Panai Island, North Palawan Block, Philippines. *Natural science research, Faculty of Integrated Arts and Sciences, the University of Tokushima*, vol. 29, p. 5–20.

Isozaki, Y. and Matsuda, T., 1980: Age of the Tamba Group along the Hozugawa "Anticline", western hills of Kyoto, Southwest Japan. *Journal of Geosciences*, *Osaka City University*, vol. 23, p. 115–134.

Isozaki, Y. and Matsuda, T., 1982: Middle and Late Triassic conodonts from bedded chert sequences in the Mino-Tamba Belt, Southwest Japan. Part 1: *Epigondolella*. *Journal of Geosciences*, *Osaka City University*, vol. 25, p. 103–136.

Isozaki, Y. and Matsuda, T., 1983: Middle and Late Triassic conodonts from bedded chert sequences in the Mino-Tamba Belt, Southwest Japan. Part 2: *Misikella* and *Parvigondolella*. *Journal of Geosciences*, *Osaka City University*, vol. 26, p. 65–86.

Katvala, E. C. and Stanley, G. D. Jr., 2008: Conodont biostratigraphy and facies correlations in a Late Triassic island arc, Keku Strait, southeast Alaska. *In*, Blodgett, R.B. and Stanley, G. D., Jr., *eds*., *The terrane Puzzle: New Perspectives on Paleontology and Stratigraphy from the North American Cordillera*, Geological Society of America Special Paper 442, p. 181–226. Geological Society of America, Boulder.

Kiliç, A. M., Plasencia, P., Ishida, K. and Hirsch, F., 2015: The case of the Carnian (Triassic) conodont genus *Metapolygnathus* Hayashi. *Journal of Earth Science*, vol. 26, p. 219–223.

Kishida, Y. and Hisada, K., 1985: Late Triassic and Early Jurassic radiolarian assemblages from the Ueno-mura area, Kato Mountains, central Japan. *Memoirs of Osaka Kyoiku University*, *Ser.III*, vol. 34, p. 103–129. (*in Japanese with English abstract*)

Kishida, Y. and Hisada, K., 1986: Radiolarian assemblages of the sambosan Belt in the western part of the Kanto Mountains, central Japan. *News of Osaka Micropaleontologists*, *Special*

Volume, no. 7, p. 25–34. (*in Japanese with English abstract*)

Kishida, Y. and Sugano, K., 1982: Radiolarian zonation of Triassic and Jurassic in Outer Side of Southwest Japan. *News of Osaka Micropaleontologists*, *Special Volume*, no. 5, p. 271–300. (*in Japanese with English abstract*)

Klets, T. V., 2005: Palaeobiogeographic zoning of Triassic seas of northeastern Asia based on conodontophoridae, *Albertiana*, vol. 32, p. 40–50.

Klets, T. V. and Kopylova, A. V., 2008: Upper Triassic conodonts from northeastern Russia: paleobiogeography, evolutional stages, biostratigraphy. *Berichte der Geologischen Bundesanstalt*, vol. 76, p. 45–49.

Koike, T., 1979: Biostratigraphy of Triassic conodonts. *In,* Inamori J. *ed*., *Biostratigraphy of Permian and Triassic Conodonts and Holothurian Sclerites in Japan*, p. 21–77. Memorial Volume of Prof. Mosaburo Kanuma, Tokyo. (*in Japanese; original title translated*)

Koike, T., 1981: Biostratigraphy of Triassic conodonts in Japan. *Science Reports of the Yokohama National University*, *Section II*, no. 28, p. 25–42.

Koike, T., 1982: Review of some platform conodonts of the Middle and Late Triassic in Japan. *Science Reports of the Yokohama University*, *Section II,* no. 29, p. 15–27.

Kolar, T., 1979: Conodonts from the Skofja Loka limestone of Smarjetna Gora. *Geologija*, vol. 22, p. 309-325.

Kovács, S., 1977: New conodonts from the North Hungarian Triassic. *Acta Mineralogica–Petrographica, Szeged*, vol. 13, p. 77–90.

Kovács, S., 1983: On the evolution of excelsa-stock in the upper Ladinian–Carnian (Conodonta,

Genus Gondolella, Triassic). *Schriftenreihe der Erdwissenschaftlichen Kommission, Österreichischen Akademie der Wissenschaften*, vol. 5, p. 107–120.

Kovács, S., 1986: Conodont-biostratigraphical and microfacies investigations in the Hungarian part of the northeastern Rudabanya Mts. *Annual Report of the Hungarian Geological Institute 1986*, p. 193–244.

Kovács, S. and Kozur, H. W., 1980: Stratigraphische Reichweite der wichtigsten Conodonten (ohne Zahnreihen-Conodonten) der Mittel- und Obertrias. *Geologisch-Paläontologische Mitteilungen Innsbruck*, vol. 10, p. 42–78.

Kovács, S., Less, G. Y., Piros, O., Reti, Z. S. and Roth, L., 1989: Triassic formations of the Aggtelek-Rubabanya mountains (north-eastern Hungary). *Acta Geologica Hungarica*, vol. 32, p. 31–63.

Kozur, H., 1972: Die Conodontengattung Metapolygnathus HAYASHI 1968 und ihr stratigraphischer Wert. *Geologisch-Paläontologische Mitteilungen Innsbruck*, vol. 2, p. 1-37.

Kozur, H., 1973: Beiträge zur Stratigraphie und Paläontologie der Trias. *Geologisch-Paläontologische Mitteilungen Innsbruck*, vol. 3, p. 1–30.

Kozur, H., 1974: Die Conodontengattung Metapolygnathus HAYASHI 1968 und ihr stratigraphischer Wert. *Geologisch-Paläontologische Mitteilungen Innsbruck*, vol. 4, p. 1–35.

Kozur, H., 2003: Integrated ammonoid-, conodont and radiolarian zonation of the Triassic. *Hallesches Jahrbuch für Geowissenschaften*, vol. 25, p. 49–79.

Kozur, H. and Mock, R., 1972: Neue Conodonten aus der Trias der Slowakei und ihre stratigrapische Bedeutung. *Geologisch-Paläontologische Mitteilungen Innsbruck*, vol. 2, p. 1–20.

Kozur, H. and Mock, R., 1991: New Middle Carnian and Rhaetian Conodonts from Hungary and the Alps. Stratigraphic Importance and Tectonic Implications for the Buda Mountains and Adjacent Areas. *Jahrbuch der Geologischen Bundesanstalt*, Band 134, p. 271–297.

Kozur, H. and Mostler, H., 1971, Probleme der Conodontenforschung in der Trias. *Geologisch-Paläontologische Mitteilungen Innsbruck*, vol. 1, p. 1–19.

Kozur, H. and Mostler, H., 1972: Die Bedeutung der Conodonten für stratigraphische und paläogeographische Untersuchungen in der Trias. *Mitteilungen der Gesellschaft der Geologie und Bergbaustudenten*, vol. 21, p. 777–810.

Kozur, H. W., Moix, P. and Ozsvárt, P., 2009: New Spumellaria (Radiolaria) from the Early Tuvalian *Spongotortilispinus moixi* Zone of southeastern Turkey, with some remarks on the age of this fauna. *Jahrbuch der Geologischen Bundesanstalt A*, Band 149, p. 25–59.

Krystyn, L., 1973: Zur Ammoniten- und Conodonten-Stratigraphie der Hallstätter Obertrias (Salzkammergut, Österreich). *Verhandlungen der Geologischen Bundesanstalt A*, Band 1, p. 113–153.

Krystyn, L., 1980: Triassic conodont localities of the Salzkammergut region (northern Calcareous Alps). *Abhandlungen der Geologischen Bundesanstalt*, Band 35, p. 61–98.

Krystyn, L., 1983: The Epidauros Section (Greece): a contribution to the conodont standard zonation of the Ladinian and Lower Carnian of the Tethys Realm. *Schriftenreihe der*

Erdwissenschaftlichen Kommission, *Österreichischen Akademie der Wissenschaften*, Band 5, p. 231–258.

Krystyn, L., 2008: An ammonoid-calibrated Tethyan conodont time scale of the late Upper Triassic. *Berichte der Geologischen Bundesanstalt*, Band 76, p. 9–11.

Krystyn, L., Bouquerel, H., Kuerchener, W., Richoz, S. and Gallet, Y., 2007: Proposal for a candidate GSSP for the base of the Rhaetian stage. *New Mexico Museum of Natural History and Science Bulletin*, no. 41, p.189–199.

Krystyn, L., Mandl, G. W. and Schauer, M., 2009: Growth and termination of the Upper Triassic platform margin of the Dachstein area (Northern Calcareous Alps, Austria). *Austrian Journal of Earth Sciences*, vol. 102, p. 23–33.

Lindström, M., 1970: A suprageneric taxonomy of the conodonts. *Lethaia*, vol. 3, p. 427–445.

Lucas, S. G., 2010: The Triassic timescale: An introduction. *Geological Society, London, Special Publications*, vol. 334, p.1–16.

Maejima, W., and Matsuda, R., 1977: Discovery of Triassic conodonts from Paleozoic strata in the northern Subbelt of the Chichibu Belt in the North of Yuasa, Wakayma Prefecture and its geological significance. *Journal of the Geological Society of Japan*, vol. 83, p. 599–600. (*in Japanese; original title translated*)

Matsuda, T. and Isozaki, Y., 1991: Well-documented travel history of Mesozoic pelagic chert in Japan: from remote ocean to subduction zone. *Tectonics*, vol. 10, p. 475–499.

Martini, R., Zaninetti, L., Abate, B., Renda, P., Doubinger, J., Rauscher, R. and Vrielynck, B., 1991: Sédimentologie et biostratigraphie de la Formation triasique Mufara (Sicile

occidentale): Foraminifères, Conodontes, Palynomorphes. *Rivista Italiana di Paleontologia e Stratigrafia*, vol. 97, p. 131–152.

Martini, R., Zaninetti, L., Villeneuve, M., Cornée, J. -J., Krystyn, L., Cirilli, S., De Wever, P., Dumitricã, P. and Harsolumakso, A., 2000: Triassic pelagic deposits of Timor: paleogeographic and sea-level implications. *Palaeogeography*, *Palaeoclimatology*, *Palaeoecology*, vol. 160, p. 123–151.

Mastandrea, A., 1995: Carnian conodonts from upper Triassic strata of the Tamarin section (San Cassiano FM., Dolomites, Italy). *Rivista Italiana di Paleontologia e Stratigrafia*, vol. 100, p. 493–506.

Mazza M., Cau A. and Rigo M., 2012a: Application of numerical cladistic analyses to the Carnian-Norian conodonts: a new approach for phylogenetic interpretations. *Journal of Systematic Palaeontology*, vol. 10, p. 401–422.

Mazza, M., Furin, S., Spötl, C. and Rigo, M., 2010: Generic turnovers of Carnian/ Norian conodonts: climatic control of competition? *Palaeogeography*, *Palaeoclimatology*, *Palaeoecology*, vol. 290, p. 120–137.

Mazza, M., Rigo, M. and Gullo, M., 2012b: Taxonomy and biostratigraphic record of the Upper Triassic conodonts of the Pizzo Mondello section (western Sicily, Italy), GSSP candidate for the base of the Norian. *Rivista Italiana di Paleontologia e Stratigrafia*, vol. 118, p. 85–130.

Mikami, T., Ishida, K. and Suzuki, S., 2008: Conodont biostratigraphy across the Carnian-Norian Boundary in the Jifukudani Creek, Tamba Terrane, SE Kyoto, Japan.

Stratigraphy, vol. 5, p. 163–178.

Mizutani, S., 1964: Superficial folding of the Paleozoic system of central Japan. *The Journal of earth sciences*, *Nagoya University*, vol. 12, p. 17–83.

Mock, R., 1971: Conodonten aus der Trias der Slowakei und ihre Verwendung in der Stratigraphie. *Geologický zborník*, vol. 22, p. 241–260.

Mock, R., 1979: *Gondolella carpathica* n. sp. eine wichtige tuvalische conodontenart. *Geologisch-Paläontologische Mitteilungen Innsbruck*, vol. 9, p. 171–174.

Mosher, L. C., 1968a: Triassic conodonts from western North America and Europe and their correlation. *Journal of Paleontology*, vol. 42, p. 895–946.

Mosher, L. C., 1968b: Evolution of Triassic platform conodonts. *Journal of Paleontology*, vol. 42, p. 947–954.

Mosher, L. C., 1970: New conodont species as Triassic guide fossils. *Journal of Paleontology*, vol. 44, p.737–742.

Mosher, L. C., 1973: Triassic conodonts from British Columbia and Northern Arctic Islands. *Geological Survey of Canada Bulletin*, vol. 222, p. 141–172.

Moix, P., Kozur, H. W., Stampfli, G. M. and Mostler, H., 2007: New paleontological, biostratigraphic and paleogeographic results from the Triassic of the Mersin Mélange, SE Turkey. *New Mexico Museum of Natural History and Science Bulletin*, no. 41, p. 282–311.

Murata, M. and Nagai, T., 1972: Discovery of conodonts from Sekkenai, Hiranai-cho, Higashi-Tsugaru-gun, Aomori Prefecture, Japan. *Prof. Jun-Ichi Iwai Memorial Volume*, p.

709–717.

Muttoni, G., Kent, D. V., Di Stefano, P., Gullo, M., Nicora, A., Tait, J. and Lowrie, W., 2001: Magnetostratigraphy and biostratigraphy of the Carnian/Norian boundary interval from the Pizzo Mondello section (Sicani Mountains, Sicily). *Palaeogeography*, *Palaeoclimatology*, *Palaeoecology*, vol. 166, p. 383–399.

Muttoni, G., Kent, D. V., Olsen, P. E., Di Stefano, P., Lowrie, W., Bernasconi, S. M. and Hernandez, F. M. 2004: Tethyan magnetostratigraphy from Pizzo Mondello (Sicily) and correlation to the Late Triassic Newark astrochronological polarity time scale. *Geological Society of America Bulletin*, vol. 116, p. 1043–1058.

Muttoni, G., Mazza, M., Mosher, D., Katz, M.E., Kent, D.V., Balini, M., 2014. A Middle–Late Triassic (Ladinian–Rhaetian) carbon and oxygen isotope record from the Tethyan Ocean. *Palaeogeography*, *Palaeoclimatology*, *Palaeoecology*, vol. 399, p. 246–259.

Nagao, H. and Matsuda, T., 1982: "Rhaetian problem" in terms of conodont biostratigraphy–A case study in bedded chert sequence at Toganoo, in northwest of Kyoto, Southwest Japan. *News of Osaka Micropaleontologists*, *Special Volume*, no. 5, p. 469–478. (*in Japanese with English abstract*)

Nakada, R., Ogawa, K., Suzuki, N., Takahashi, S. and Takahashi, Y., 2014: Late Triassic compositional changes of aeolian dusts in the pelagic Panthalassa: Response to the continental climatic change. *Palaeogeography*, *Palaeoclimatology*, *Palaeoecology*, vol. 393, p. 61–75.

Nakaseko, K. and Nishimura, A., 1979: Upper Triassic Radiolaria from Southwest Japan.

Science Reports, *College of General Education*, *Osaka University*, vol. 28, p. 61–109.

Nicoll, R. S. and Foster, C. B., 1994: Late Triassic conodont and palynomorph biostratigraphy and conodont thermal maturation, North West Shelf, Australia. *AGSO Journal of Australian Geology and Geophysics*, vol. 15, p. 101–11.

Nicora, A., Balini, M., Bellanca, A., Bertinelli, A., Bowring, S. A., Di Stefano, P., Dumitrica, P., Guaiumi, C., Gullo, M., Hungerbuehler, A., Levera, M., Mazza, M., McRoberts, C. A., Muttoni, G., Preto, N. and Rigo, M., 2007: The Carnian/Norian boundary interval at Pizzo Mondello (Sicani Mountains, Sicily) and its bearing for the definition of the GSSP of the Norian Stage. *Albertiana*, vol. 36, p. 102–129.

Noyan, Ö. F. and Kozur, H. W., 2007: Revision of the Late Carnian–Early Norian conodonts from the Stefanion section (Argolis, Greece) and their palaeobiogeographic implications. *Neues Jahrbuch für Geologie und Paläontologie*, *Abhandlungen*, Band 245, p. 159–178.

Noyan, Ö. F. and Vrielynck, B., 2000: Importance of morphogenetic analysis in taxonomy: an example from Triassic platform conodonts. *Neues Jahrbuch für Geologie und Paläontologie, Monatshefte 2000*, p. 577–594.

Oda, H. and Suzuki, H., 2000: Paleomagnetism of Triassic and Jurassic red bedded chert of the Inuyama area, central Japan. *Journal of Geophysical Research*, vol. 105, p. 25743–25767.

O'Dogherty, L., Carter, E. S., Gorican, S. and Dumitrica, P., 2010: Triassic radiolarian biostratigraphy. *Geological Society*, *London*, *Special Publications*, vol. 334, p. 163–200.

Ogg, J. G., 2012: Triassic. *In*, Gradstein, F. M., Ogg, J. G., Schmitz, M. D. and Ogg, G. M. *eds.*, *The Geological Time Scale 2012*, vol. 2, p. 681–730. Elsevier, New York.

Okami, K., Endo, S. and Murata, M., 1978: Discovery of Triassic conodonts from the chert pebbles of the Tertiary conglomerates of Joban coal-field (The conglomerates of the eastern terrain of Abukuma plateau, part 2). *Journal of the Geological Society of Japan*, vol. 84, p. 87–90. (*in Japanese; original title translated*)

Onoue, T., Sato, H., Nakamura, T., Noguchi, T., Hidaka, Y., Shirai, N., Ebihara, M., Osawa, T., Hatsukawa, Y., Toh, Y., Koizumi, M., Harada, H., Orchard M. J. and Nedachi, M., 2012: A deep-sea record of impact apparently unrelated to mass extinction in the Late Triassic. *Proceedings of the National Academy of Sciences of the USA*, vol. 109, p. 19134–19139.

Onoue, T., Sato, H., Yamashita, D., Ikehara, M., Yasukawa, K., Fujinaga, K., Kato, Y. and Matsuoka, A., 2016a: Bolide impact triggered the Late Triassic extinction event in equatorial Panthalassa. *Scientific Reports*, doi: 10.1038/srep29609.

Onoue, T, Zonneveld, J.-P., Orchard, M. J., Yamashita, M., Yamashita, K., Sato, H. and Kusaka, S., 2016b, Paleoenvironmental changes across the Carnian/Norian boundary in the Black Bear Ridge section, British Columbia, Canada. *Palaeogeography*, *Palaeoclimatology*, *Palaeoecology*, vol. 441, p. 721–733.

Orchard, M. J., 1983: *Epigondolella* populations and their phylogeny and zonation in the Norian (Upper Triassic), *Fossils and Strata*, vol. 15, p. 177–192.

Orchard, M. J., 1991a: Late Triassic conodont biochronology and biostratigraphy of the Kunga Group, Queen Charlotte Islands, British Columbia. *In,* Woodsworth, G.W., *ed.*, *Evolution and Hydrocarbon Potential of the Queen Charlotte Basin*, *British Columbia.* p. 173–193. *Geological Survey of Canada*, Ottawa.

Orchard M. J., 1991b: Upper Triassic conodont biochronology and new index species from the Canadian Cordillera. *Geological Survey of Canada Bulletin*, vol. 417, p. 299–335.

Orchard, M. J. 1994: Late Triassic (Norian) conodonts from Peru. *In*, Stanley, G. D., Jr., *ed*., *Paleontology and Stratigraphy of Triassic to Jurassic rocks of the Peruvian Andes.*, *Palaeontographica Abteilung A*, vol. 233, p. 203–208.

Orchard, M. J., 2005: Multielement conodont apparatuses of Triassic Gondolelloidea. *Special Papers in Palaeontology*, no. 73, p. 73–101.

Orchard, M. J., 2006: Late Paleozoic and Triassic conodont faunas of Yukon Territory and northern British Columbia and implications for the evolution of the Yukon-Tanana terrane. *In*, Colpron, N. and Nelson, J.L. *eds*., *Paleozoic Evolution and Metallogeny of Pericratonic Terranes at the Ancient Pacific Margin of North America, Canadian and Alaskan Cordillera*, p. 229–260. Geological Association of Canada, Canada.

Orchard, M. J., 2007a: New conodonts and zonation, Ladinian-Carnian boundary beds, British Columbia, Canada. *New Mexico Museum of Natural History and Science Bulletin*, no. 41, p. 321–330.

Orchard, M. J., 2007b: Conodont lineages from the Carnian-Norian boundary at Black Bear Ridge, northeast British Columbia. *New Mexico Museum of Natural History and Science Bulletin*, no. 41, p. 331–332.

Orchard, M. J., 2007c: A proposed Carnian-Norian boundary GSSP at Black Bear Ridge, northeast British Columbia, and a new conodont framework for the boundary interval. *Albertiana*, vol. 36, p. 130–141.

Orchard, M. J., 2013: Five new genera of conodonts from the Carnian-Norian Boundary beds, northeast British Columbia, Canada. *New Mexico Museum of Natural History and Science Bulletin*, no. 61, p. 445–457.

Orchard, M. J., 2014: Conodonts from the Carnian-Norian Boundary (Upper Triassic) of Black Bear Ridge. *New Mexico Museum of Natural History and Science Bulletin*, no. 64, p. 1–139.

Orchard, M. J. and Balini, M., 2007: Conodonts from the Ladinian-Carnian boundary beds of South Canyon, New Pass, Nevada, USA. *New Mexico Museum of Natural History and Science Bulletin*, no. 41, p. 333–340.

Orchard, M. J., Zonneveld, J-P., Johns, M. J., McRoberts, C. A., Sandy, M. R., Tozer, E. T. and Carrelli, G. G., 2001: Fossil succession and sequence stratigraphy of the Upper Triassic and Black Bear Ridge, northeast B.C., and a GSSP prospect for the Carnian-Norian boundary. *Albertiana*, vol. 25, p. 10–22.

Orchard, M. J., Carter, E. S., Lucas, S. G and Taylor, D.G., 2007a: Rhaetian (Upper Triassic) conodonts and radiolarians from New York Canyon, Nevada, USA. *Albertiana*, vol. 35, p. 59–65.

Orchard, M. J., Whalen, P. A., Carter, E. S. and Taylor, H. J., 2007b: Latest Triassic conodonts and radiolarian-bearing successions in Baja California Sur. *New Mexico Museum of Natural History and Science Bulletin*, no. 41, p. 355–365.

Rigo, M., De Zanche, V., Gianolla, P., Mietto, P., Preto, N. and Roghi, G., 2005: Correlation of Upper Triassic sections throughout the Lagonegro Basin. *Bollettino della Società*

Geologica Italiana, vol. 124, p. 293–300.

Rigo, M., Preto, N., Roghi, G., Tateo, F. and Mietto, P., 2007: A rise in the Carbonate Compensation Depth of western tethys in the Carnian (Late Triassic): Deep-water evidence for the Carnian pluvial event. *Palaeogeography*, *Palaeoclimatology*, *Palaeoecology*, vol. 246, p. 188–205.

Rigo M., Preto, N., Franceschi, M. and Guaiumi, C., 2012: Stratigraphy of the Carnian-Norian Calcari con Selce Formation in the Lagonegro Basin, Southern Apennines. *Rivista Italiana di Paleontologia e Stratigrafia*, vol. 118, p. 143–154.

Rigo, M., Bertinelli, A., Concheri, G., Gattolin, G., Godfrey, L., Katz, M., Maron, M., Mietto, P., Muttoni, G., Sprovieri, M., Stellin, F. and Zaffani, M., 2016: The Pignola-Abriola section (southern Apennines, Italy): a new GSSP candidate for the base of the Rhaetian Stage. *Lethaia*, vol. 49, p. 287–306.

Sashida, K., Nishimura, H., Igo, H., Kazama, S. and Kamata, Y., 1993: Triassic radiolarian faunas from Kiso-fukushima, Kiso Mountains, central Japan. *Science reports of the Institute of Geoscience*, *University of Tsukuba*. *Section B*, vol. 4, p. 77–97.

Sato, T., Murata, M. and Yoshida, H., 1986, Triassic to Jurassic radiolarian biostratigraphy in the southern part of Chichibu terrain of Kyushu, Japan. *News of Osaka Micropaleontologists*, *Special Volume*, no. 7, p. 9–23. (*in Japanese with English abstract*)

Sato, H., Onoue, T., Nozaki, T. and Suzuki, K., 2013: Osmium isotope evidence for a large Late Triassic impact event. *Nature Communications*, doi: 10.1038/ncomms3455.

Schlager, W. and Schöllnberger, W., 1974: Das Prinzip stratigraphischer Wenden in der

Schichtfolge der Nördlichen Kalkalpen. *Mitteilungen der Österreichischen Geologischen Gesellschaft*, vol. 66–67, p. 165–193.

Shibuya, H. and Sasajima, S., 1986: Paleomagnetism of red cherts: A case-study in the Inuyama area, central Japan. *Journal of Geophysical Research,* vol. 91, p. 14105–14116.

Simms, M. J. and Ruffell, A. H., 1989: Synchroneity of climatic change and extinctions in the Late Triassic. *Geology*, vol. 17, p. 265–268.

Sugiyama, K., 1992: Lower and Middle Triassic radiolarians from Mt. Kinkazan, Gifu Prefecture, central Japan. *Transactions and Proceedings of the Palaeontological Society of Japan*, *New Series*, no. 167, p. 1180–1223.

Sugiyama, K., 1997: Triassic and Lower Jurassic radiolarian biostratigraphy in the siliceous claystone and bedded chert units of the southeastern Mino Terrane, Central Japan. *Bulletin of the Mizunami Fossil Museum*, vol. 24, p.79–193.

Sugiyama, K., Kawakami, S. and Takano, M., 2001: Aerial photograph and stratigraphic correlation of the Triassic to Lower Jurassic siliceous claystone and bedded chert units of the Inuyama and Hisuikyo areas, central Japan. *News of Osaka Micropaleontologists*, *Special Volume*, no. 12, p. 145–157. (*in Japanese with English abstract*)

Sweet, W. C., Mosher, L. C., Clark, D. L., Collinson, J. W. and Hasenmueller, W. A., 1971, Conodont biostratigraphy of the Triassic. *In*, Sweet, W. C. and Bergstrome, S. M. *eds*., *Symposium on conodont biostratigraphy, Geological Society of America, Memoirs*, no. 127, p. 441–465.

Tatge, U., 1956: Conodonten aus dem germanischen Muschelkalk. *Paläontologische Zeitschrift*,

Band 30, p. 108–147.

Uno, K., Yamashita, D., Onoue, T. and Uehara, D., 2015: Paleomagnetism of Triassic bedded chert from Japan for determining the age of an impact ejecta layer deposited on peri-equatorial latitudes of the paleo-Pacic Ocean: A preliminary analysis. *Physics of the Earth and Planetary Interiors*, vol. 249, p. 59–67.

Vrielynck, B., 1981: Conodontes du Trias perimediterraneen. Systematique, stratigraphie. *Documents des Laboratoires de Géologie de Lyon*, vol. 97, p. 1–301.

Wakita, K., 1988: Origin of chaotically mixed rock bodies in the Early Jurassic to Early Cretaceous sedimentary complex of the Mino terrane, central Japan. *Bulletin of the Geological Survey of Japan*, vol. 39, p. 675–757.

Yao, A., 1982: Middle Triassic to Early Jurassic radiolarians from the Inuyama area, central Japan. *Journal of Geosciences*, *Osaka City University*, vol. 25, p. 53–70.

Yao, A., 1990: Triassic and Jurassic radiolarians. *In*, Ichikawa, K., Mizutani, S., Hara, I., Hada, S. and Yao, A. *eds*., *Pre-Cretaceous Terrane of Japan, publication of IGCP project no. 224*, p. 329–345. Nippon Insatsu, Osaka.

Yao, A., Matsuda, T. and Isozaki, Y., 1980: Triassic and Jurassic radiolarians from the Inuyama area, central Japan. *Journal of Geosciences*, *Osaka City University*. vol. 23, p. 135–154.

Yao, A., Matsuoka, A. and Nakatani, T., 1982: Triassic and Jurassic radiolarian assemblages in Southwest Japan. *News of Osaka Micropaleontologists*, *Special Volume*, no. 5, 27–43. (*in Japanese with English abstract*)

Yoshida, H., 1986: Upper Triassic to Lower Jurassic radiolarian biostratigraphy in

Kagamigahara City, Gifu Prefecture, central Japan. *Journal of Earth sciences*, *Nagoya University*, vol. 34, p. 1–21, pls. 1–17.

Ziegler, W., 1977: *Catalogue of Conodonts 3*, 574 p. E. Schweizerbart'sche Verlagsbuchhandlung, Science Publishers, Stuttgart.

Zonneveld, J. P., Beatty, T. W., Williford, K. H., Orchard, M. J. and McRoberts, C.A., 2010: Stratigraphy and sedimentology of the lower Black Bear Ridge section, British Columbia: candidate for the base-Norian GSSP. *Stratigraphy*, vol. 7, p. 61–82.

Figure captions.

Figure 1. A, B, Locality map of the Inuyama area in central Japan. **C,** Geological map of the Inuyama area with location of the studied section (Modified after Onoue *et al*., 2012).

Figure 2. Sketch maps showing the location of the measured point in a bedded chert succession of the section N (**A,** modified after Sato *et al*., 2013) and Q (**B**).

Figure 3. Lithology and stratigraphic occurrence of conodonts and radiolarians in the section N.

Figure 4. Lithology and stratigraphic occurrence of conodonts and radiolarians in the section Q.

Figure 5. Calibration of Upper Triassic conodont and radiolarian zonations in Inuyama area,

and their correlation with the conodont and ammonoid zonations in British Columbia (Orchard, 1991, 2007a, 2014).

Figure 6. Calibration of Upper Triassic conodont and radiolarian zonations in Inuyama area, and their correlation with the conodont zonations in Japan (Koike, 1981; Ishida and Hirsch, 2001; Mikami *et al*., 2008).

Figure 7. SEM images of Upper Triassic conodonts from the section N and Q. **1,** *Carnepigondolella* aff. *samueli* (Orchard, 1991b), KMSP-100001, sample N-130; **2, 3,** *Carnepigondolella zoae* (Orchard, 1991b), KMSP-100002, sample QU1-170, KMSP-100003, sample N-115; **4, 5,** *Epigondolella quadrata* Orchard, 1991b, beta morphotype, KMSP-100004, sample QU2-346, KMSP-100005, sample QU2-221; **6,** *Epigondolella rigoi* Kozur, 2007, KMSP-100006, sample NCU-430; **7,** *Epigondolella triangularis* (Budurov, 1972), KMSP-100007, sample NCU-430; **8,** *Kraussodontus ludingtonensis* Orchard, 2013, KMSP-100008, sample N-117; **9,** *Epigondolella spatulata* (Hayashi, 1968), KMSP-100009, sample N-H. For 1–9: a, upper view; b, lateral view; c, lower view. Scale bar = 300 μm.

Figure 8. SEM images of Upper Triassic conodonts from the section N and Q. **1–3,** *Kraussodontus roberti* Orchard, 2014, alpha morphotype, KMSP-100010, sample N-121, KMSP-100011, sample NCU-70, KMSP-100012, sample QU1-88; **4,** *Mockina bidentata*

(Mosher, 1968a) from the original plates of Onoue *et al*. (2016a: Supplementary Figure S12), KMSP-100013, sample NHR-45; **5,** *Mockina bidentata* (Mosher, 1968a), KMSP-100014, sample NHR-70; **6, 7,** *Mockina elongata* (Orchard, 1991b), KMSP-100015, sample NHR-42, KMSP-100016, sample NHR-56; **8, 9,** *Mockina mosheri* (Kozur and Mostler, 1971) morphotype A, KMSP-100017, sample NHR-72, KMSP-100018, sample QU3-163; **10,** *Mockina mosheri* (Kozur and Mostler, 1971) morphotype B, KMSP-100019, sample QU3-163; **11,** *Mockina postera* (Kozur and Mostler, 1971) from the original plates of Onoue *et al*. (2016a: Supplementary Figure S12), KMSP-100020, sample NHR-40; **12,** *Mockina slovakensis* (Kozur, 1972), KMSP-100021, sample NHR-112; **13, 14,** *Epigondolella spiculata* (Orchard, 1991b), KMSP-100022, sample NCU-541, KMSP-100023, sample NCU-541. For 1–14: a, upper view; b, lateral view; c, lower view. Scale bar = 300 μm.

Figure 9. SEM images of Upper Triassic conodonts from the section N and Q. **1,** *Mockina* aff. *zapfei* (Kozur, 1972), KMSP-100024, sample QU3-163; **2, 3,** *Mockina* sp. indet. A, KMSP-100025, sample NHR-130, KMSP-100026, sample NHR-55; **4–6,** *Mockina* sp. indet. B, KMSP-100027, sample QU3-163, KMSP-100028, sample NHR-42, KMSP-100029, sample NHR-57; **7,** *Neogondolella* cf. *liardensis* Orchard, 2007a, KMSP-100030, sample NCL-185; **8,** *Paragondolella auriformis* (Kovács, 1977), KMSP-100031, sample NCU24; **9,** *Paragondolella*? *tadpole* (Hayashi, 1968), KMSP-100032, sample NCU-18. For 1–9: a, upper view; b, lateral view; c, lower view.

Scale bar = 300 μm.

Figure 10. SEM images of Upper Triassic conodonts from the section N and Q. **1, 2,** *Paragondolella inclinata* (Kovács, 1977), KMSP-100033, sample NCL-2, KMSP-100034, sample NCL-128 ; **3,** *Paragondolella* aff. *praelindae* Kozur, 2003, KMSP-100035, sample NCL-2; **4,** *Parvigondolella andrusovi* Kozur and Mock, 1972, KMSP-100036, sample NHR-53; **5,** *Parvigondolella* aff. *vrielyncki* Kozur and Mock, 1991, KMSP-100037, sample NHR-53; **6, 7,** *Primatella orchardi* (Kozur, 2003), KMSP-100038, sample N-130, KMSP-100039, sample NCU-186; **8, 9,** *Quadralella carpathica* (Mock, 1979), KMSP-100040, sample QU2-62, KMSP-100041, sample N-115. For 1–9: a, upper view; b, lateral view; c, lower view. Scale bar = 300 μm.

Figure 11. SEM images of Upper Triassic conodonts from the section N and Q. **1, 2,** *Quadralella noah* (Hayashi, 1968), KMSP-100042, sample NCU-70, KMSP-100043, sample QU1-88; **3, 4,** *Quadralella tuvalica* (Mazza and Rigo, 2012), KMSP-100044, sample QU2-63, KMSP-100045, sample N-130; **5, 6,** *Quadralella postlobata* Orchard, 2014, KMSP-100046, sample NCU-130, KMSP-100047, sample N-121; **7,** *Quadralella* sp. indet A, KMSP-100048, sample NCU-131. For 1–7: a, upper view; b, lateral view; c, lower view. Scale bar = 300 μm.

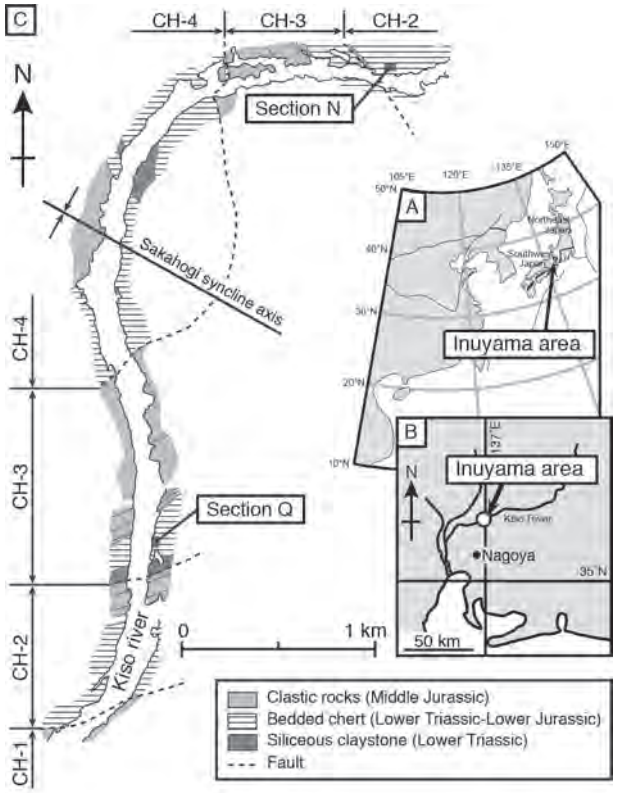
C
CH-4
CH-3
CH-2
N
Section N
Sakahogi syncline axis
CH-4
CH-3
CH-2
CH-1
Section Q
Kiso river
0
1 km
A
Inuyama area
B
Inuyama area
N
Kiso River
Nagoya
35°N
50 km
Clastic rocks (Middle Jurassic)
Bedded chert (Lower Triassic-Lower Jurassic)
Siliceous claystone (Lower Triassic)
Fault

Fig. 1

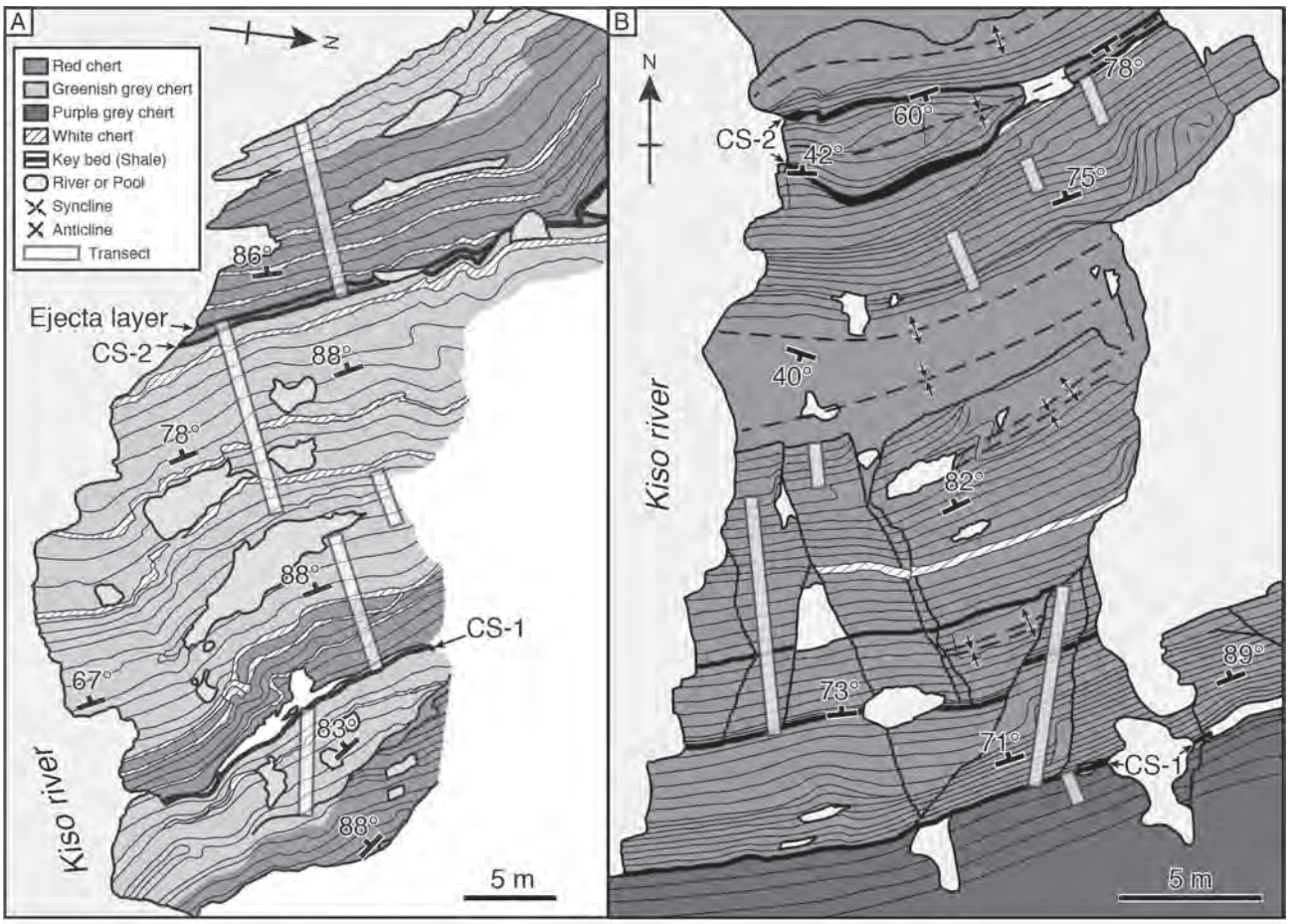
A
N
Red chert
Greenish grey chert
Purple grey chert
White chert
Key bed (Shale)
River or Pool
Syncline
Anticline
Transect
86°
Ejecta layer
CS-2
88°
78°
88°
CS-1
67°
83°
88°
Kiso river
5 m
B
N
78°
60°
CS-2
42°
75°
40°
Kiso river
82°
89°
73°
71°
CS-1
5 m

Fig. 2

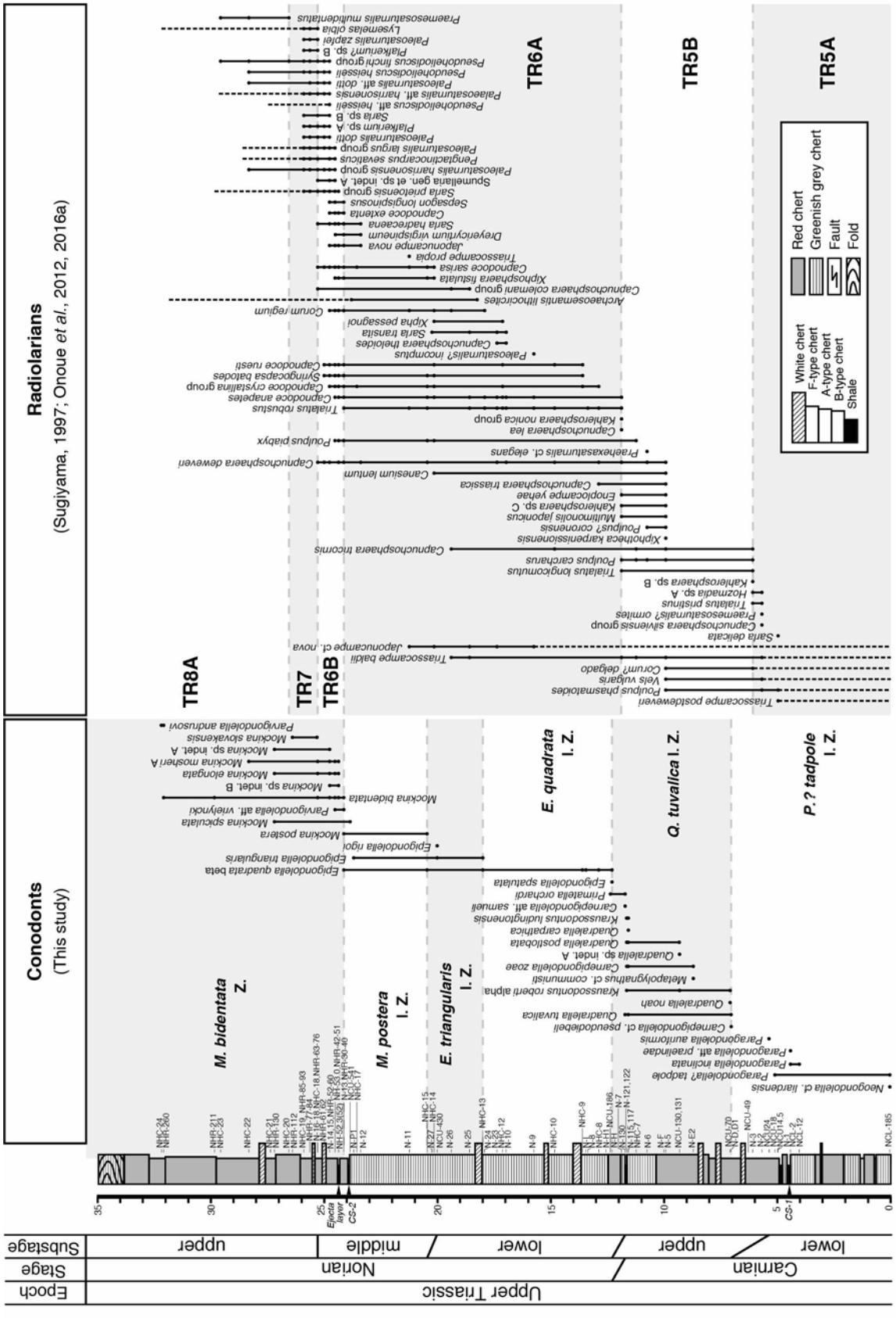
Radiolarians
(Sugiyama, 1997; Onoue et al., 2012, 2016a)
Conodonts
(This study)
TR8A
TR7
TR6B
TR6A
TR5B
TR5A
White chert
F-type chert
A-type chert
B-type chert
Shale
Red chert
Greenish grey chert
Fault
Fold
Trassocampe postlewerl
Pouplus phasmatoides
Vals vulgaris
Corum? delgado
Trassocampe balcli
Japonucampe ct. nova
Sarla delicata
Capnuchosphaera silvensis group
Paramesosaturnalis? ornilles
Trialatus pristinus
Hozmadia sp. A
Kahlerosphaera sp. B
Trialatus longicornutus
Pouplus carcharus
Capnuchosphaera tricornis
Xiphotheca karpenssionensis
Pouplus? coronensis
Multimonolis japonicus
Kahlercampe sp. C
Enoplocampe yehae
Capnuchosphaera trassica
Canesium lentum
Praehexasaturnalis cf. elegans
Capnuchosphaera dewerwerl
Pouplus plalyx
Capnuchosphaera lea
Kahlerosphaera nonica group
Trialatus robustus
Capnodoce anapetes
Capnodoce crystallina group
Syringocapsa balodes
Capnodoce ruesli
Paleosaturnalis? incomptus
Capnuchosphaera theloides
Sarla transita
Xiphe pessagnoi
Corum regium
Archaeosemantis lithocirtes
Capnuchosphaera coleman group
Xiphosphaera fistulata
Capnodoce sarisa
Trassocampe profia
Japonucampe nova
Dreyercyrtium virgispinum
Sarla hadreaena
Capnodoce exlenta
Sepsagon longispinosus
Sarla pretoriensis group
Spumellara gen. et sp. indet. A
Paleosaturnalis harrisonensis group
Pentactinocarpus sevaticus
Paleosaturnalis largus group
Paleosaturnalis dotti
Plalkerium sp. A
Sarla sp. B
Pseudohelidiscus aff. heissell
Palaeosaturnalis aff. harrisonensis
Paleosaturnalis aff. dotti
Pseudohelidiscus heissell
Pseudohelidiscus finchi group
Plalkerium? sp. B
Paleosaturnalis zapfel
Lysemelas olivia
Praemesosaturnalis multidentatus
M. bidentata Z.
M. postera I. Z.
E. triangularis I. Z.
E. quadrata I. Z.
Q. tuvalica I. Z.
P.? tadpole I. Z.
Mockina dentata
Mockina postera
Epigondolella rigoi
Epigondolella quadrata beta
Epigondolella triangularis
Mockina spiculata
Parvigondolella aff. vrielynckl
Mockina bidentata
Mockina sp. indet. B
Mockina elongata
Mockina mosheri A
Mockina sp. indet. A
Mockina slovakensis
Parvigondolella andrusovi
Neogondolella cf. liardensis
Paragondolella? tadpole
Paragondolella inclinata
Paragondolella aff. praelinda
Paragondolella auritomis
Carnepigondolella cf. pseudodiebeli
Quadralella tuvalica
Quadralella noah
Krassodontus roberti alpha
Metapolygnathus cf. communisti
Carnepigondolella zoae
Quadralella sp. indet. A
Quadralella postlobata
Quadralella carpathica
Krassodontus lulingtonensis
Carnepigondolella aff. samueli
Primatella orcharci
Epigondolella spatulata
Epigondolella quadrata beta
Epigondolella triangularis
Epigondolella rigoi
Mockina postera
Mockina spiculata
Parvigondolella aff. vrielynckl
Mockina bidentata
Mockina sp. indet. B
Mockina elongata
Mockina mosheri A
Mockina sp. indet. A
Mockina slovakensis
Parvigondolella andrusovi
NHC-24
NHR-200
NHR-211
NHC-23
NHC-22
NHC-21
NHR-130
NHC-20
NHR-112
NHC-19
NHR-85-93
NHC-18
NHR-74-84
N-14,15
NHR-52-60
NHR-53.0
NHR-42-51
NHC-17
NHR-63-76
NHR-69-40
N-P1
N-12
N-11
NHC-15
NHC-14
N-27
NCU-430
N-26
N-25
NHC-13
N-24
N-23
NHC-12
N-10
N-9
NHC-10
NHC-9
N-8
NHC-8
N-H1
N-130
N-H2
N-H3
NCU-166
N-7
N-121,122
N-6
N-F
N-5
NCU-130,131
N-E2
NCU-70
NCU-01
NCU-49
N-3
N-2,24
NCU-115
N-1
NCL-2
NCL-12
NCL-185
35
30
25
20
15
10
5
0
Ebicla layer
CS-2
CS-1
Upper Triassic
Epoch
Norian
Carnian
Stage
upper
middle
lower
upper
lower
Substage

Fig. 3

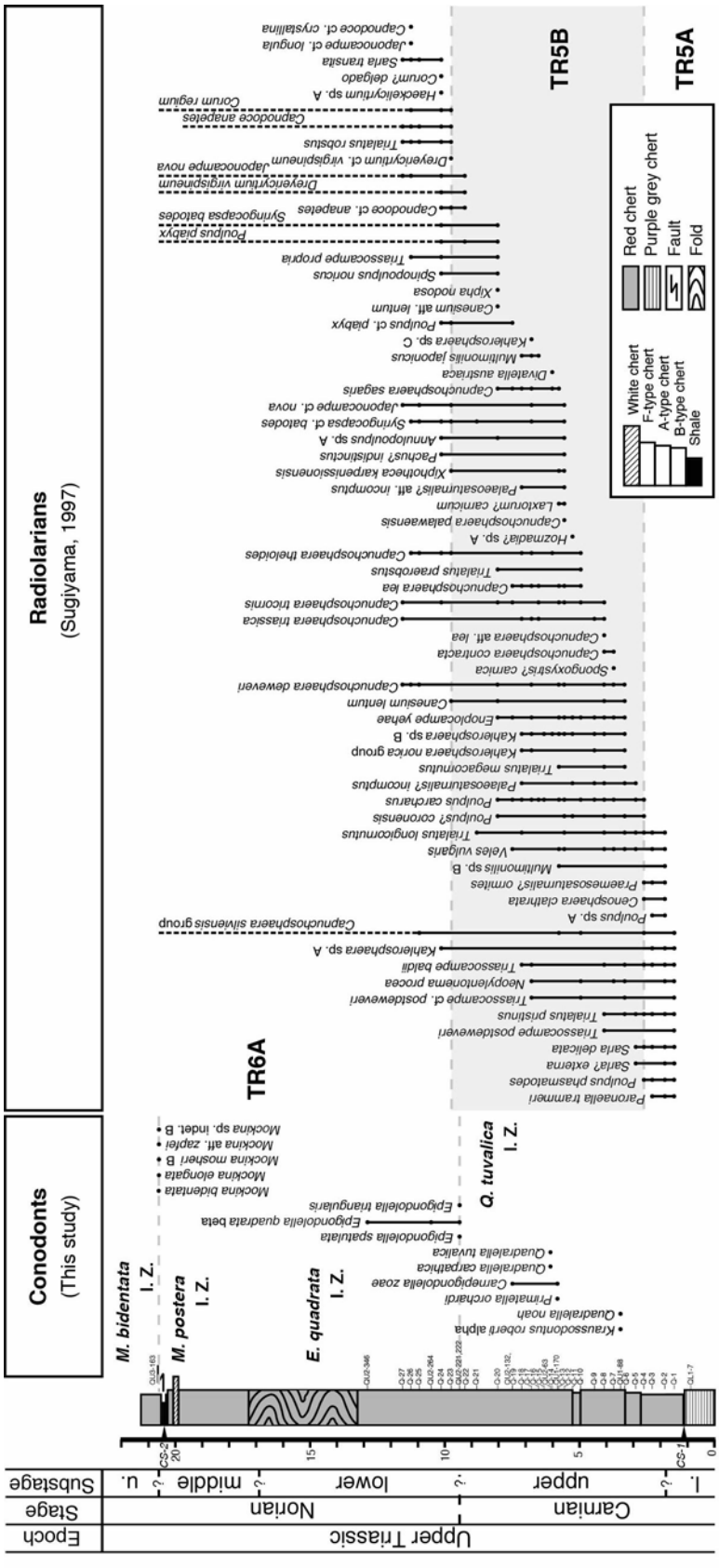
Radiolarians
(Sugiyama, 1997)
Conodonts
(This study)
TR6A
TR5B
TR5A
Red chert
Purple grey chert
Fault
Fold
White chert
F-type chert
A-type chert
B-type chert
Shale
Paronella trammeri
Poulpus phasmatodes
Sarla? externa
Sarla delicata
Triassocampe postdeweveri
Trialatus pristinus
Triassocampe cf. postdeweveri
Neopylentonema procea
Triassocampe baldi
Kahlerosphaera sp. A
Capnuchosphaera silvensis group
Poulpus sp. A
Cenosphaera clathrata
Praemesosaturnalis? ormiles
Multimonilis sp. B
Velos vulgaris
Trialatus longicornutus
Poulpus? coronensis
Poulpus carcharus
Palaeosaturnalis? incomptus
Trialatus megacornutus
Kahlerosphaera norica group
Kahlerosphaera sp. B
Enoplocampe yehae
Canesium lentum
Capnuchosphaera deweveri
Spongoxystris? carnica
Capnuchosphaera contracta
Capnuchosphaera aff. lea
Capnuchosphaera trassica
Capnuchosphaera tricornis
Capnuchosphaera lea
Trialatus praerobstus
Capnuchosphaera thelolides
Hozmadia? sp. A
Capnuchosphaera palawanensis
Laxtorum? carnicum
Palaeosaturnalis? aff. incomptus
Xiphotheca karpentissionensis
Pachus? indistinctus
Annulopoulpus sp. A
Syringocapsa cf. batoides
Japonocampe cf. nova
Capnuchosphaera sagaris
Divatella australica
Multimonilis japonicus
Kahlerosphaera sp. C
Poulpus cf. plabyx
Canesium aff. lentum
Xipha nodosa
Spinopoulpus noricus
Triassocampe propria
Poulpus plabyx
Capnodoce cf. anapetes
Syringocapsa batoides
Dreyercyrtium virgispineum
Dreyercyrtium cf. virgispineum
Japonocampe nova
Trialatus robstus
Capnodoce anapetes
Corum regium
Haeckelicyrtium sp. A
Corum? delgado
Sarla transita
Japonocampe cf. longula
Capnodoce cf. crystallina
Mockina bidentata
Mockina elongata
Mockina mosheri B
Mockina aff. zaplei
Mockina sp. indet. B
Epigondolella triangularis
Epigondolella quadrata beta
Epigondolella spatulata
Quadralella tuvalica
Quadralella carpathica
Carnepigondolella zoae
Primatella orchardi
Quadralella noah
Krausseodontus robertl alpha
M. bidentata I. Z.
M. postera I. Z.
E. quadrata I. Z.
Q. tuvalica I. Z.
Epoch
Stage
Substage
Upper Triassic
Norian
Carnian
lower
middle
upper
u.
l.
?
20
15
10
5
0
CS-2
CS-1

Fig. 4

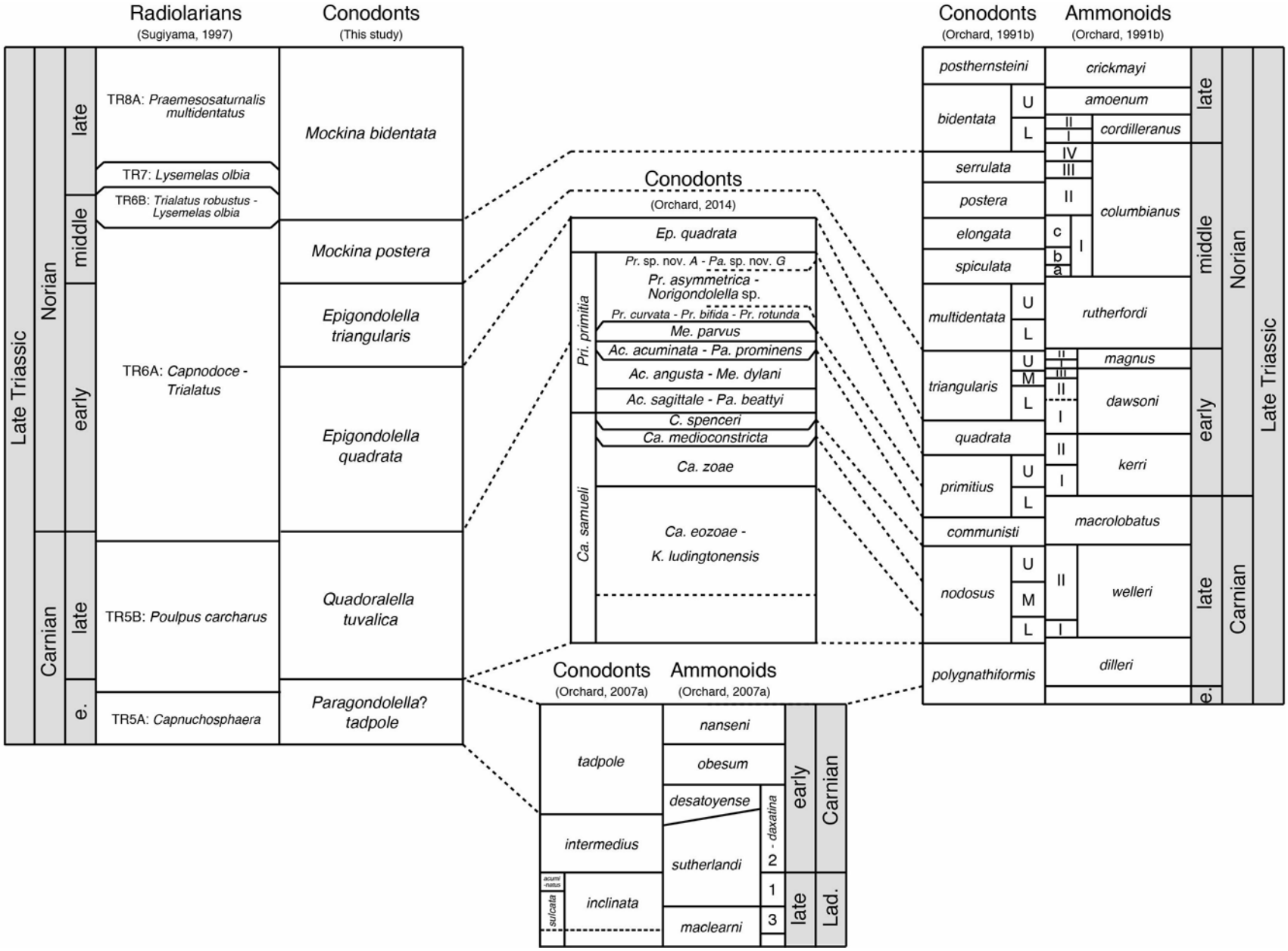
Radiolarians
(Sugiyama, 1997)
Conodonts
(This study)
Late Triassic
Norian
Carnian
late
middle
early
late
e.
TR8A: Praemesosaturnalis multidentatus
TR7: Lysemelas olbia
TR6B: Trialatus robustus - Lysemelas olbia
TR6A: Capnodoce - Trialatus
TR5B: Poulpus carcharus
TR5A: Capnuchosphaera
Mockina bidentata
Mockina postera
Epigondolella triangularis
Epigondolella quadrata
Quadoralella tuvalica
Paragondolella? tadpole
Conodonts
(Orchard, 2014)
Ep. quadrata
Pr. sp. nov. A - Pa. sp. nov. G
Pr. asymmetrica - Norigondolella sp.
Pr. curvata - Pr. bifida - Pr. rotunda
Me. parvus
Ac. acuminata - Pa. prominens
Ac. angusta - Me. dylani
Ac. sagittale - Pa. beattyi
C. spenceri
Ca. mediocostricta
Ca. zoae
Ca. eozoae - K. ludingtonensis
Pri. primitia
Ca. samueli
Conodonts
(Orchard, 2007a)
Ammonoids
(Orchard, 2007a)
tadpole
intermedius
inclinata
sulcata
acuminatus
nanseni
obesum
desatoyense
sutherlandi
maclearni
- daxatina
1
2
3
early
late
Carnian
Lad.
Conodonts
(Orchard, 1991b)
Ammonoids
(Orchard, 1991b)
posthernsteini
bidentata
serrulata
postera
elongata
spiculata
multidentata
triangularis
quadrata
primitius
communisti
nodosus
polygnathiformis
U
M
L
crickmayi
amoenum
cordilleranus
columbianus
rutherfordi
magnus
dawsoni
kerri
macrolobatus
welleri
dilleri
IV
III
II
I
c
b
a
late
middle
early
late
e.
Norian
Carnian
Late Triassic

Fig. 5

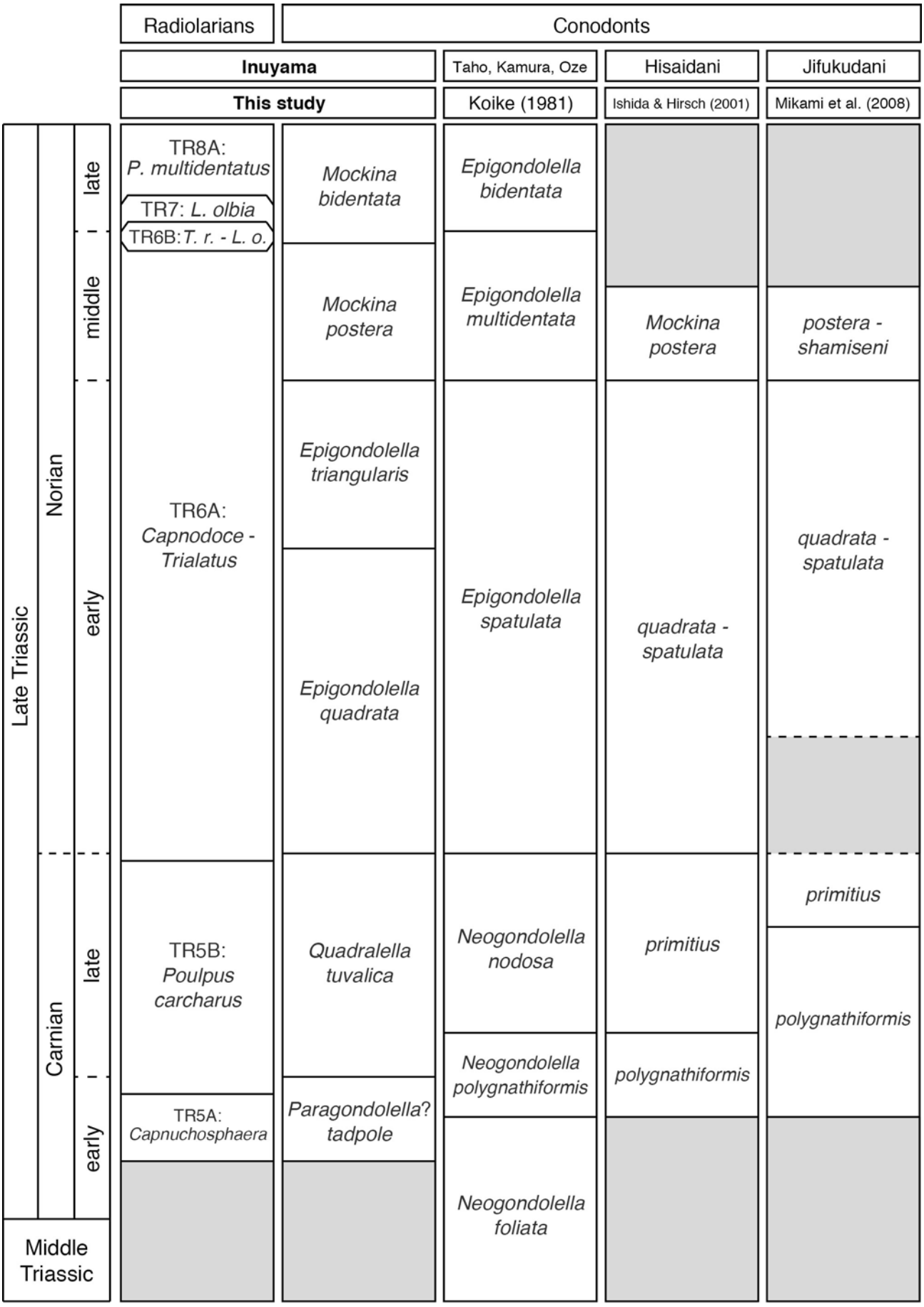
Radiolarians
Conodonts
Inuyama
Taho, Kamura, Oze
Hisaidani
Jifukudani
This study
Koike (1981)
Ishida & Hirsch (2001)
Mikami et al. (2008)
Late Triassic
Norian
Carnian
Middle Triassic
late
middle
early
late
early
TR8A: P. multidentatus
TR7: L. olbia
TR6B: T. r. - L. o.
TR6A: Capnodoce - Trialatus
TR5B: Poulpus carcharus
TR5A: Capnuchosphaera
Mockina bidentata
Mockina postera
Epigondolella triangularis
Epigondolella quadrata
Quadralella tuvalica
Paragondolella? tadpole
Epigondolella bidentata
Epigondolella multidentata
Epigondolella spatulata
Neogondolella nodosa
Neogondolella polygnathiformis
Neogondolella foliata
Mockina postera
quadrata - spatulata
primitius
polygnathiformis
postera - shamiseni
quadrata - spatulata
primitius
polygnathiformis

Fig. 6

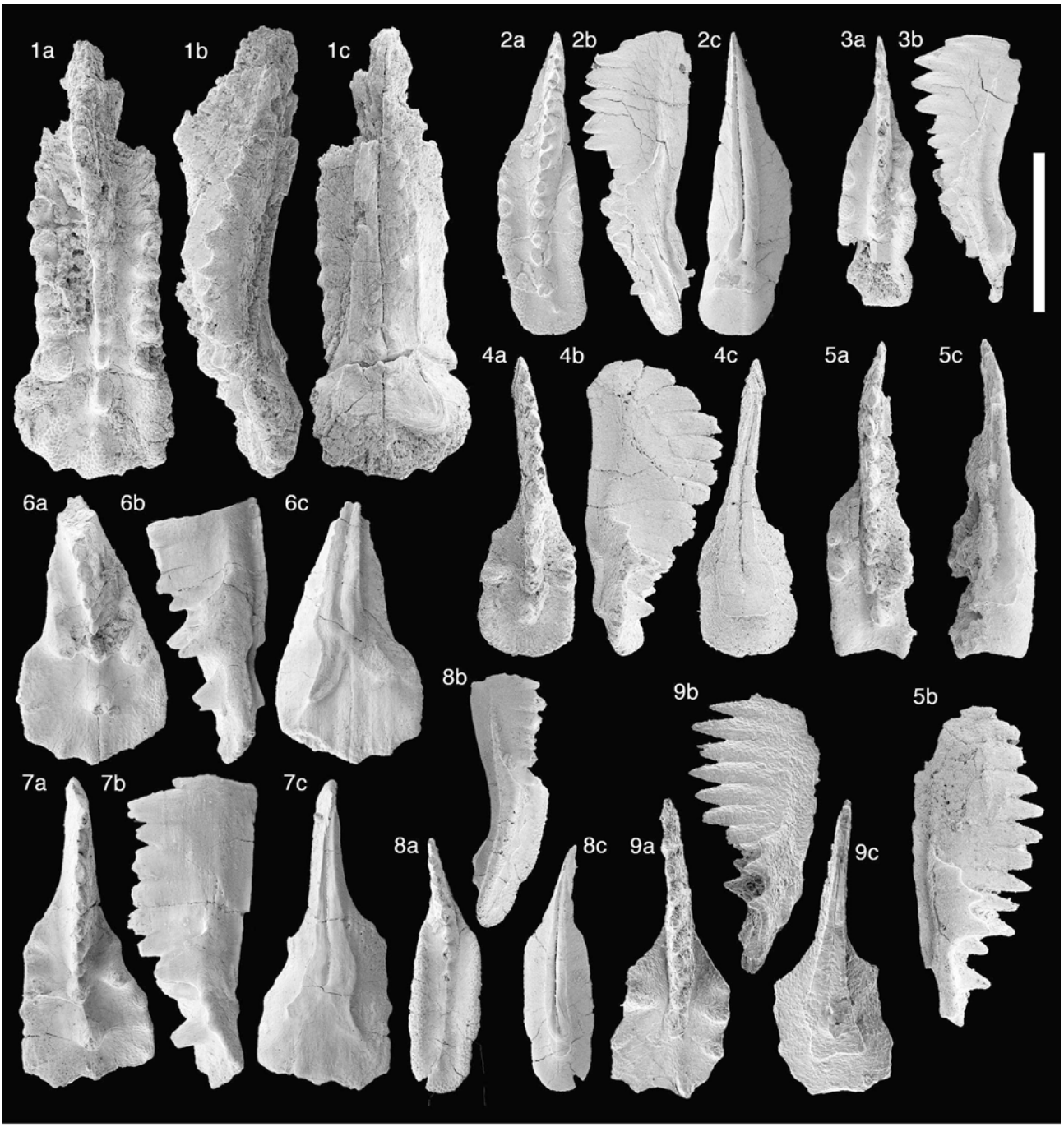
1a
1b
1c
2a
2b
2c
3a
3b
4a
4b
4c
5a
5c
6a
6b
6c
8b
9b
5b
7a
7b
7c
8a
8c
9a
9c

Fig. 7

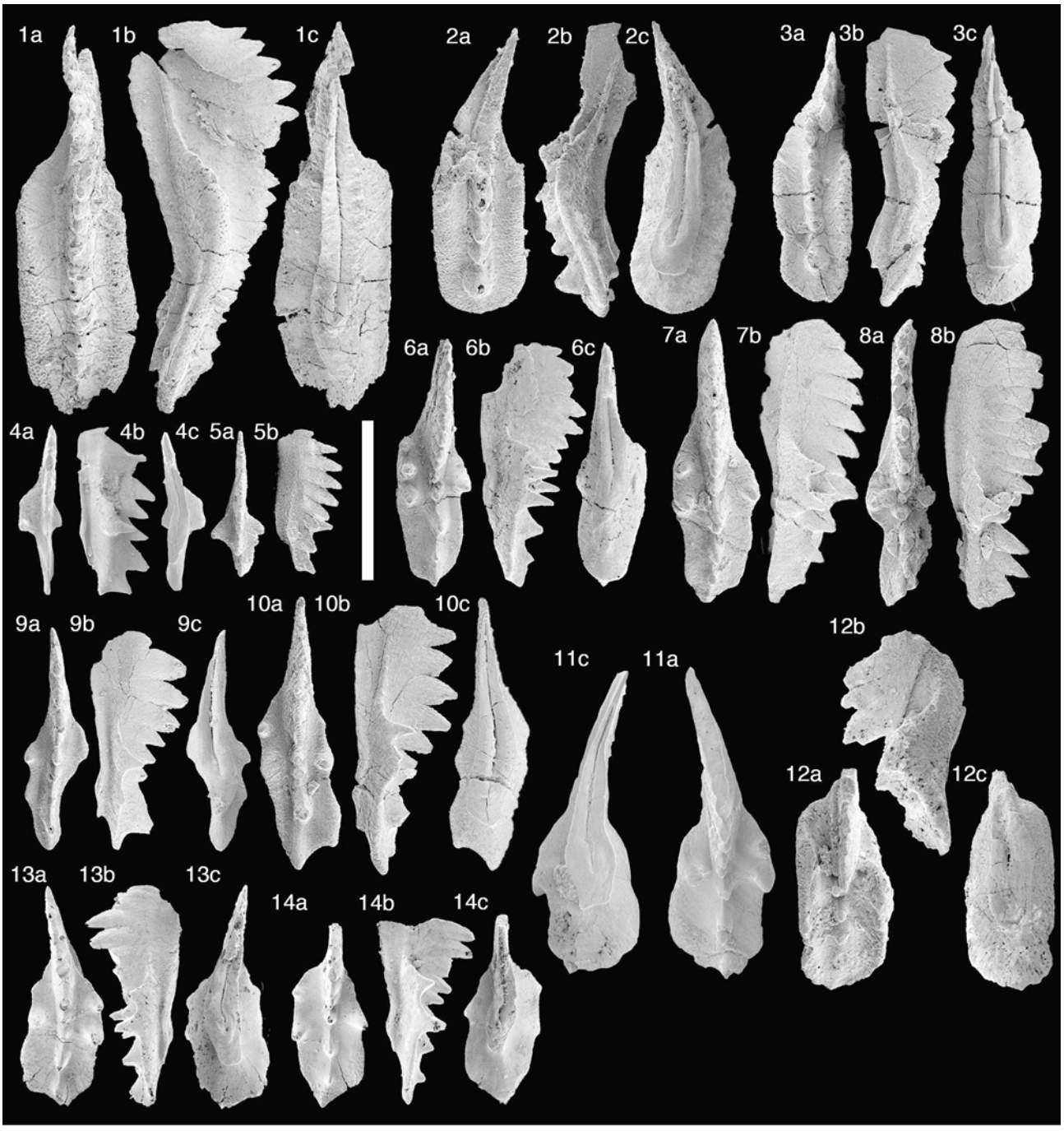
1a
1b
1c
2a
2b
2c
3a
3b
3c
4a
4b
4c
5a
5b
6a
6b
6c
7a
7b
8a
8b
9a
9b
9c
10a
10b
10c
11c
11a
12b
12a
12c
13a
13b
13c
14a
14b
14c

Fig. 8

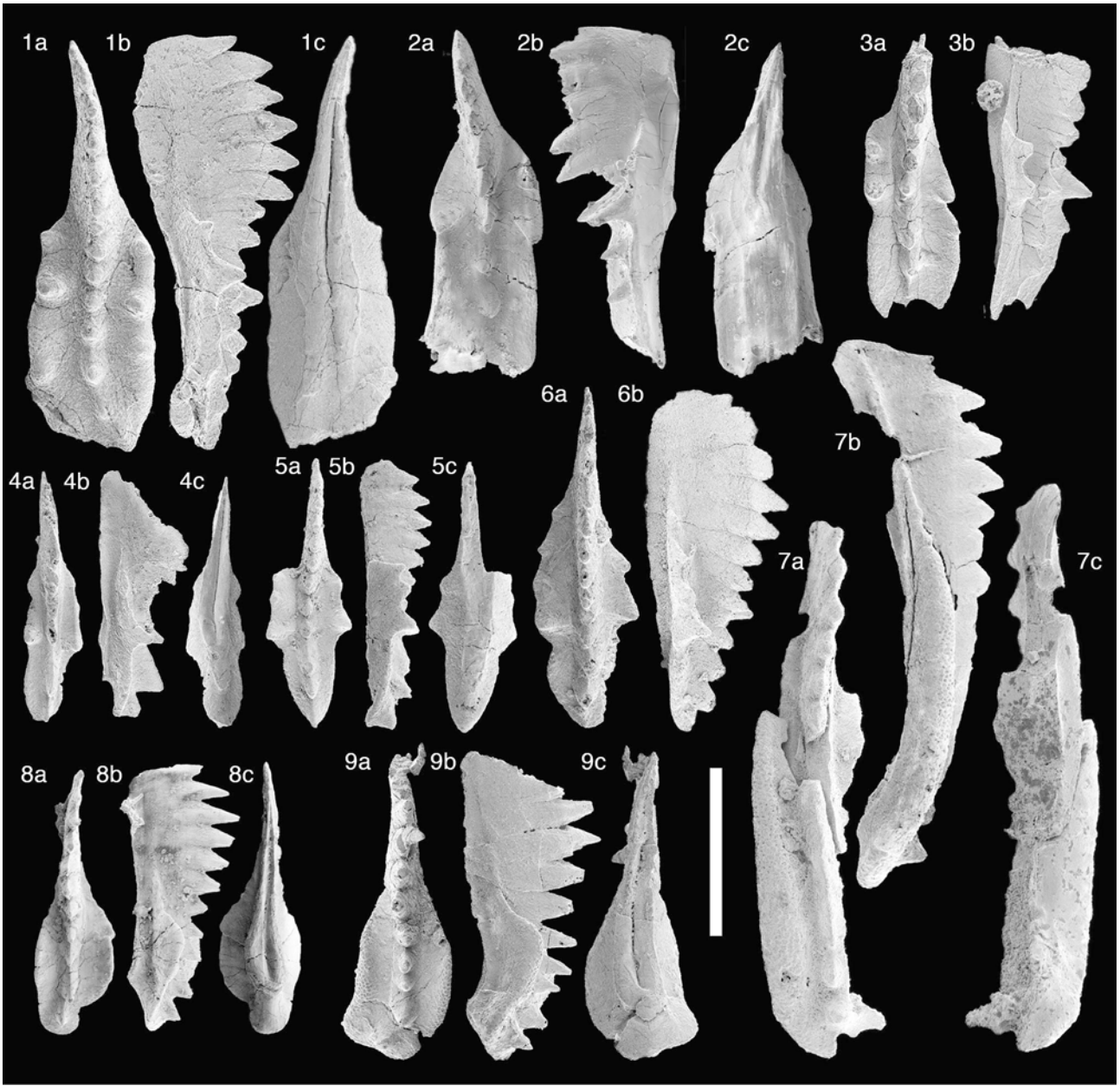
1a
1b
1c
2a
2b
2c
3a
3b
4a
4b
4c
5a
5b
5c
6a
6b
7a
7b
7c
8a
8b
8c
9a
9b
9c

Fig. 9

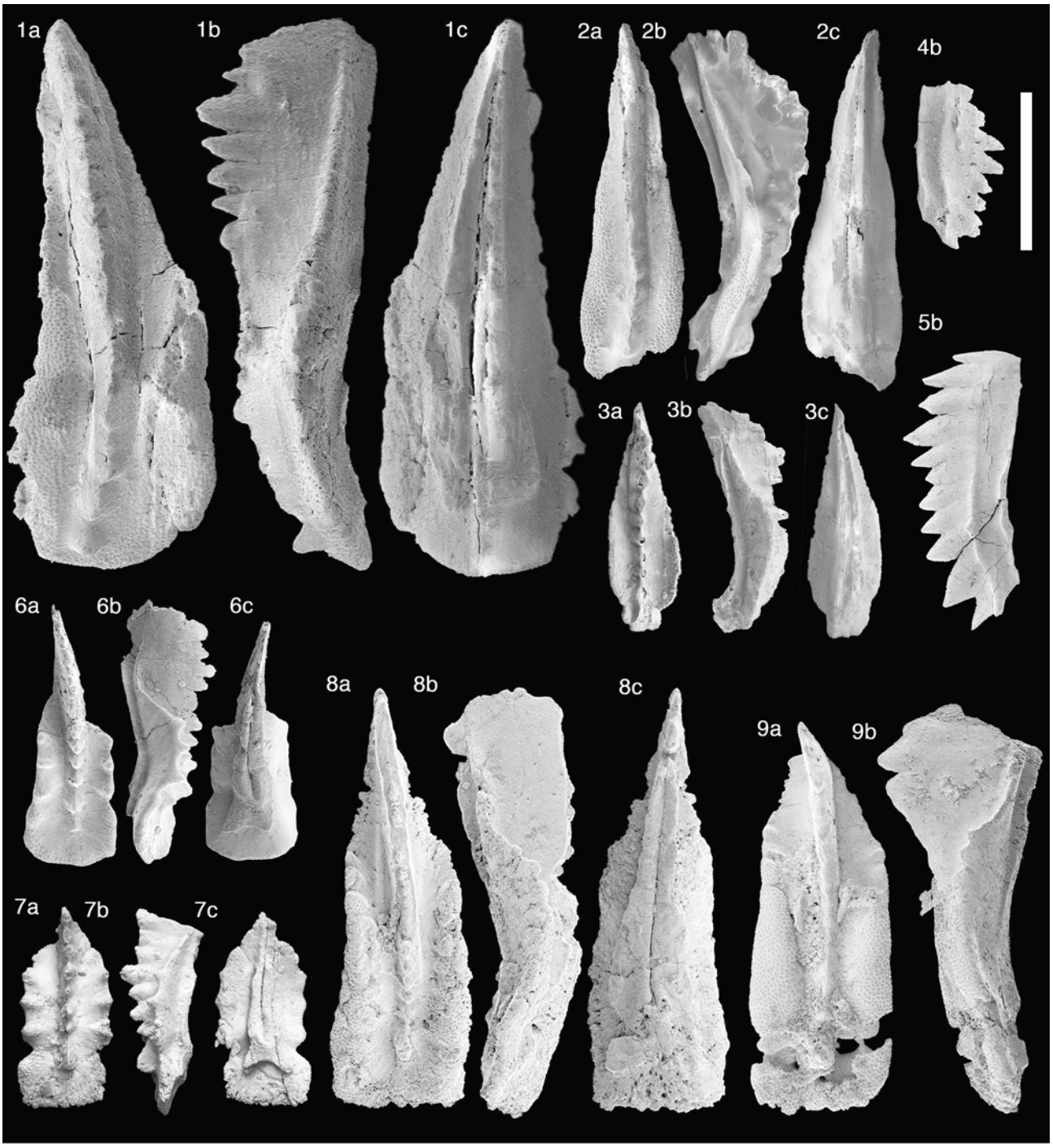

Fig. 10

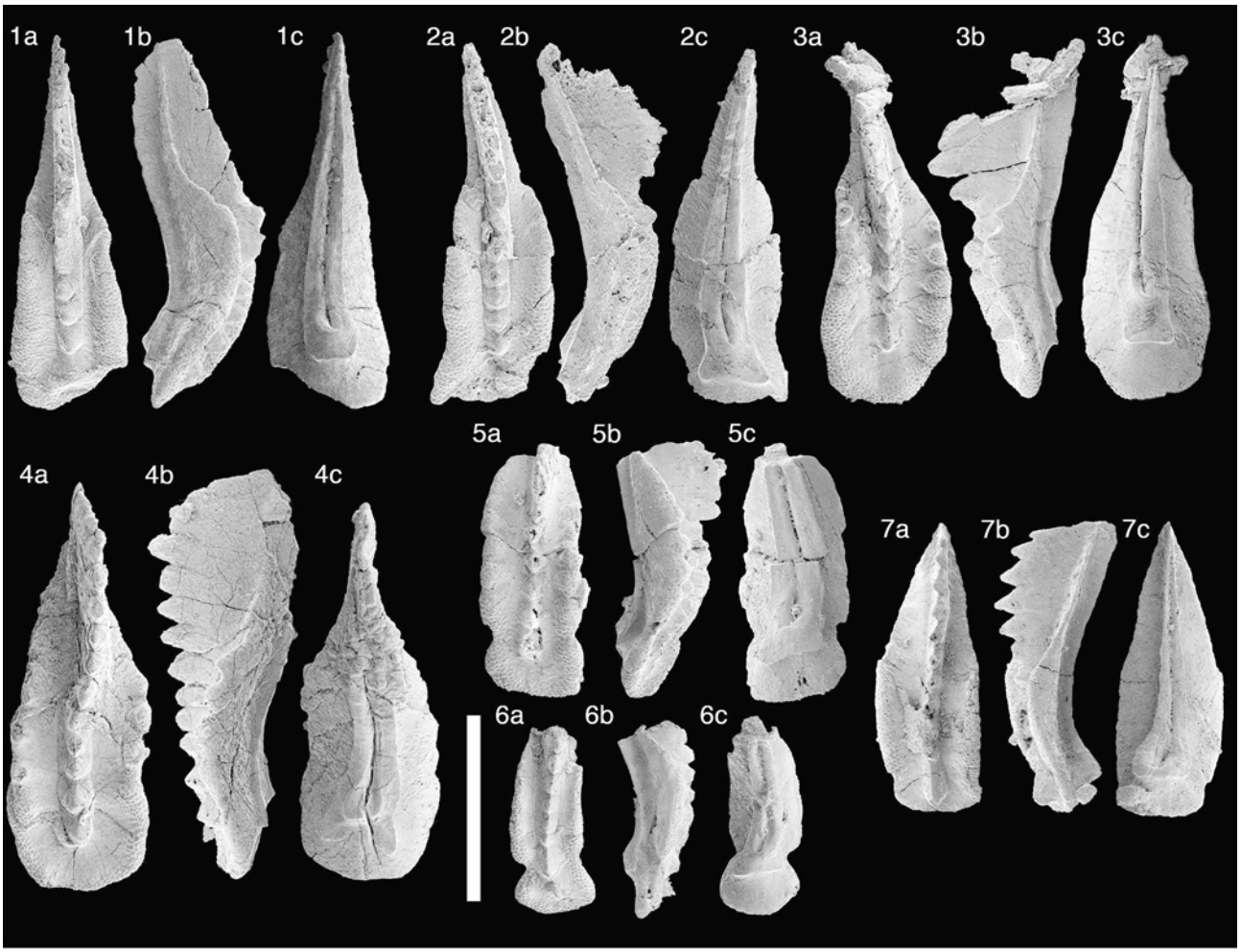

Fig. 11